SHEAR PERFORMANCE OF SUPACEE SECTIONS WITH OPENINGS : NUMERICAL STUDIES

Kajaharan Thirunavukkarasu
Institute of Technology, University of Moratuwa, Homagama, Sri Lanka

Elilarasi Kanthasamy
Faculty of Engineering and Environment, Northumbria University, Newcastle upon Tyne, UK

Keerthan Poologanathan
Faculty of Engineering and Environment, Northumbria University, Newcastle upon Tyne, UK

Konstantinos Daniel Tsavdaridis
School of Civil Engineering, Faculty of Engineering and Physical Sciences, University of Leeds, UK

Perampalam Gatheeshgar
Faculty of Engineering and Environment, Northumbria University, Newcastle upon Tyne, UK

Sivayokesvarasarma Hareindirasarma
Faculty of Engineering, University of Jaffna, Jaffna, Sri Lanka.

Alex McIntosh
Faculty of Engineering and Environment, Northumbria University, Newcastle upon Tyne, UK

Abstract:

Cold-Formed Steel (CFS) sections provide many design and construction sophistications including lightweight and high strength-to-weight ratio. The SupaCee section was introduced to CFS industry due to its cost effectiveness, enhanced strength, better structural performance and high stiffness. Introduction of SupaCee sections lead to investigations of web crippling, flexural and shear behaviour of the sections. However, structural behaviour of SupaCee sections with web openings has not been addressed to date. Hence, this study intends to analyse the shear behaviour of SupaCee sections with web openings. Previous shear test results of SupaCee sections and Lipped Channel Beam (LCB) sections with openings were validated with developed FE models. An extensive parametric study was accomplished considering various geometric parameters such as depth, yield strength, thickness and web opening ratios. Since the

results of the detailed study determined that existing design equations were over conservative, new design equations with reduction factor were proposed to predict the ultimate shear capacity of SupaCee sections with web openings. Moreover, the shear capacities of SupaCee sections were compared with shear capacities of similar dimensioned LCB sections. A web opening ratio of 0.2 is recommended, considering the ability to regain the shear capacity of plain LCB sections, as well as the availability of web openings in order to accommodate the services.

Keywords: Cold-formed Steel, SupaCee sections, Web openings, Lipped Channel section, Finite element modelling, Shear strength, Shear reduction factor

1 Introduction

Cold-formed steel (CFS) has been utilised extensively compared to hot-rolled steel in the modern building sector due to its inherent qualities and benefits: high strength, lightweight, cost-effective, faster construction, and easier transportation. CFS sections can be utilised as floor joists, roof trusses, roof purlins and partition walls, due to the wide variety of available shapes and sizes. Fig. 1 illustrates the different CFS sections and their general applications. However, CFS sections are continuously subjected to detailed investigations with respect to structural performance enhancement, material efficiency and innovative ideas. In the process, different cross-sections were introduced and studied in detail for certain structural applications. On that note, innovative SupaCee steel profiles were introduced to the Australian construction industry by BlueScope Lysaght (BlueScope Steel Ltd., Melbourne, Australia) and the University of Sydney [1]. As illustrated in Fig. 2, the SupaCee steel sections have a web with four stiffeners, which makes them extremely strong. Steel sections with web stiffeners and curved lips are considered more cost-effective, whilst also providing enhanced strength than ordinary channel sections. The SupaCee steel sections can provide better bending, bearing and shear capacities, due to their additional curved lips and longitudinal web stiffeners [2]. Therefore, SupaCee sections are often utilised as purlins in roof and wall systems.

Several research studies have examined the bending, shear strength, and behaviour of sections having longitudinal web stiffeners without web holes [3-7]. Pham and Hancock [3] used the spline finite strip method (SFSM) to explore the shear buckling of CFS sections with a single rectangular web stiffener and they found that the depth and breadth of the stiffener were the most essential variables for improving the shear buckling stress. According to the findings of Pham and Hancock's [3] investigation, stiffeners can have a considerable influence on the shear buckling stress of sections up to a certain limit of stiffener depth-to-web depth ratio. Later,

Pham et al. [4] examined the numerical shear buckling assessment of CFS sections with web stiffeners, including rectangular and triangular. However, they stated that using SFSM instead of the Finite Element Method (FEM) decreases the complexity of the computation, yet the SFSM still necessitates substantial calculations. Furthermore, web stiffeners only have a minimal impact on reducing distortional buckling stress, but it does improve shear buckling stress in rectangular and triangular web stiffener cases. Therefore, Pham et al. [5] conducted a study on the shear design for sections with web stiffeners using the Direct Strength Method (DSM), and the strength of sections in pure shear using FEM was compared with DSM strength equations. They stated that the DSM equations were well-matched, which allows for the FEM findings to be reduced due to the simplified boundary conditions than in the tests. Similarly, Pham et al. [6] and Pham and Hancock [7] performed experimental and numerical investigations, respectively on longitudinally stiffened web channels subject to shear. The results from the FEA and experiment were plotted against DSM curves in both instances and prequalified sections with longitudinally stiffened sections were proposed.

Moreover, the concept of shear buckling on CFS with holes was initiated by Rockey et al. [8] in 1969. The research [8] study was based on the effects of circular openings on the square shear webs. However, Pham [9] in 2017, analysed the shear buckling coefficients of plate and channel sections with square and circular openings and proposed shear buckling coefficients by using the SFSM method. Pham [9] compared shear buckling coefficients of perforated square plates with the traditional results provided by Rockey et al. [8] for circular holes and pointed out that when hole sizes were large shear buckling coefficients dropped drastically and non-linearly, whereas for smaller openings there were only slight deviations. Also, Pham et al. [10] proposed an alternative method based on the DSM approach to predict shear capacities of CFS sections with openings. Shear buckling coefficients were derived by them to predict the shear buckling forces which were then included in to the DSM equation.

(a) Application of CFS as floor bearers

(b) Application of CFS as purlins

(c) Application of CFS as rafters

(d) Application of CFS as joists

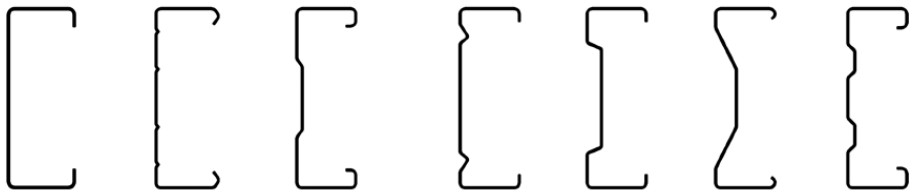

(e) Various CFS profiles applied to the above applications

Fig. 1: Profiles of different CFS sections and their applications [6, 11]

In past research studies, the experimental investigation and finite element analysis of a high strength cold-formed SupaCee section under shear, and combined bending and shear without web holes were carried out [12-15]. However, the determination of effective widths becomes more difficult when sections become more complicated, with several web stiffeners and return lips, as anticipated for SupaCee sections. Therefore, another experimental program, which is referred as the shear test series (V-series), combined bending and shear (MV-series) and bending only (M-series) for SupaCee sections was conducted in order to better understand the DSM approach of high strength cold-formed channel sections subject to shear[12,15]. Currently, there are only two primary design methodologies available for CFS members; Australian/New Zealand Standard (AS/NZS) [16] for cold-formed steel structures and Specification of the American Iron and Steel Institute (AISI 2016) [17] for cold-formed steel structural members. For CFS design, the DSM is a viable alternative to the Effective Width Method (EWM) because of its advantages, such as the ability to account for the behaviour of

intricate geometries adequately (e.g. sections with web stiffeners) and better applicability in designing [5].

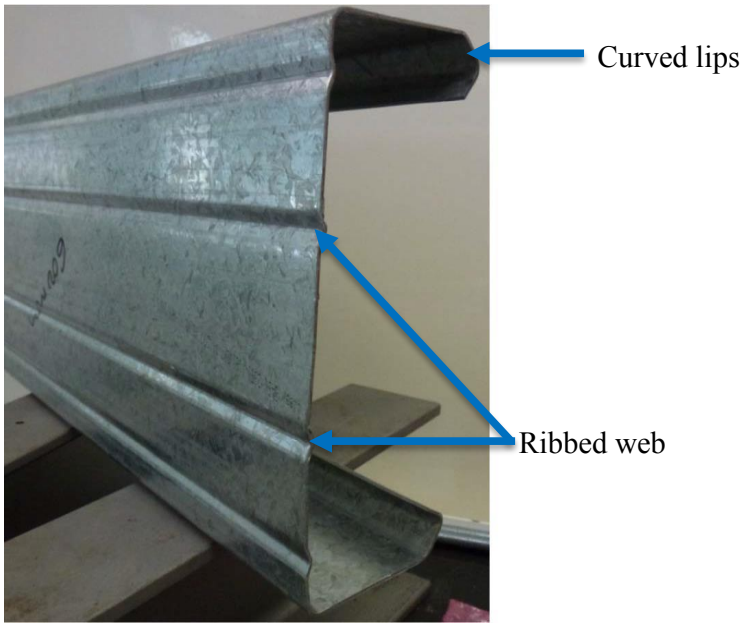

Fig. 2. SupaCee section's profile [18]

Recently, Sundararajah et al. [2, 18] investigated the web crippling behaviour of SupaCee sections using experimental and numerical analyses under one-flange and two-flange loading conditions, without web holes. Moreover, Sundararajah et al. [2, 18] stated that the SupaCee sections with web stiffeners have less web crippling capacity, whereas the web crippling capacity of SupaCee sections was reduced by around 15% as a result of localized failures under interior two-flange (ITF) loading. However, the shear behaviour of SupaCee sections with web opening is unknown. Since, SupaCee section could replace many CFS sections considering its merits and CFS sections with web openings are generally manufactured to allow access the building services such as electrical, heating and plumbing in walls and ceilings of a building, it is necessary to examine the SupaCee section with web openings. Hence, this research was performed to address that research gap, and finite element investigations of SupaCee sections with openings are detailed in this study and a suitable shear reduction factor due to the holes in the web area is later proposed. In addition, the results were compared with similar LCB sections, and SupaCee sections with web openings were recommended to replace the plain LCB sections.

2 Numerical analysis

2.1 Overview

A detailed Finite Element (FE) model has been generated to investigate the shear behaviour of SupaCee section with web openings employing ABAQUS [19] simulating the experimental set up consisting similar material characteristics, load applications, boundary conditions and geometrical and mechanical parameters. FE models were created as two sections: SupaCee beam and the Web Side Plate (WSP). The cross-section of the beam was created using symmetric dimensions with respect to middle surface offset definition. Definition of thickness, extrusion and assignment of section properties were processed to create the model initially. The aspect ratio was selected as 1.0 while developing the models to ensure predominant shear failure in the section and web openings were created at the shear span centre in both sides. Tie constraint was employed to attach the WSPs to the SupaCee section at the two end supports as well as in the mid span. Then, loading and supporting boundary conditions were applied to WSP. The WSPs prevents the direct application of the load and end boundary conditions to specimen. The developed numerical model setup is illustrated in Fig. 3. The simulation process was followed by the model generation, which comprises two steps: Linear perturbation analysis or eigenvalue buckling analysis to get buckling modes and nonlinear analysis to obtain the shear capacity and failure modes. Nonlinear analysis was performed after including the geometric imperfections by using the static Riks method.

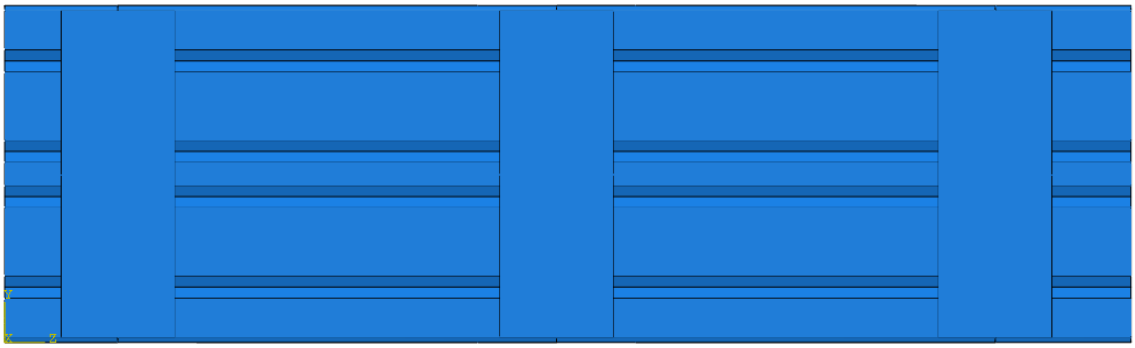

(a) Assembly of beam and WSP

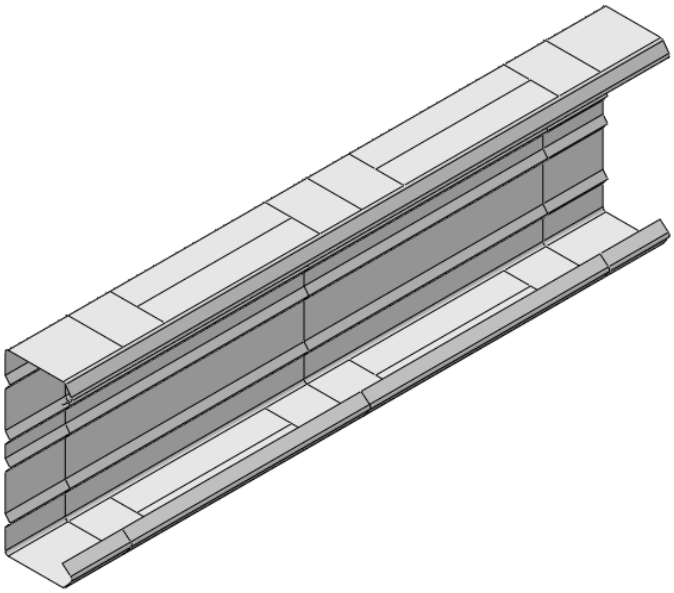

(b) Beam

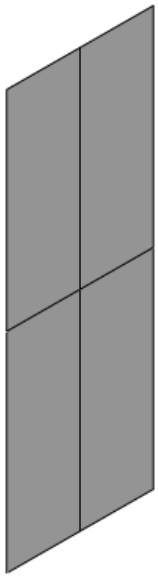

(c) WSP

Fig. 3: Developed SupaCee FE model and Web Side Plate

2.2 Element type and mesh refinement

Since the thickness (t= 1 mm, 2 mm & 2.5 mm) of SupaCee sections is negligible considering other dimensions (depth of the section (d) = 150 mm, 200 mm & 250 mm, width of the section ((B) = 50 mm, 65 mm & 75mm), S4R shell element was chosen. S4R element denotes three translational and rotational degrees of freedom (DOF) for each node. Concurrently, three-dimensional quadrilateral (R3D4) element type was selected for WSP from the rigid element type library of ABAQUS to replicate the actual characteristics such as undeformable, high strength and stiffness.

Once element formulation was done, proper refined mesh arrangement was considered in order to obtain accurate numerical values. Based on the previous research [2, 18, 20], as well as mesh

sensitivity analysis, an appropriate mesh size of 5 mm × 5 mm was selected for SupaCee flat section, 1 mm × 5 mm for corner regions of SupaCee section and 10 mm × 10 mm for WSP [20]. Finer mesh (1 mm × 5 mm) was chosen as the curvature of corner regions should be modelled accurately in order to avoid any strength loss. Whereas, WSP mesh arrangement (10 mm × 10 mm) was comparatively coarser as the results would not be obtained from WSP. Fig. 4 shows the mesh refinement of the section and WSP.

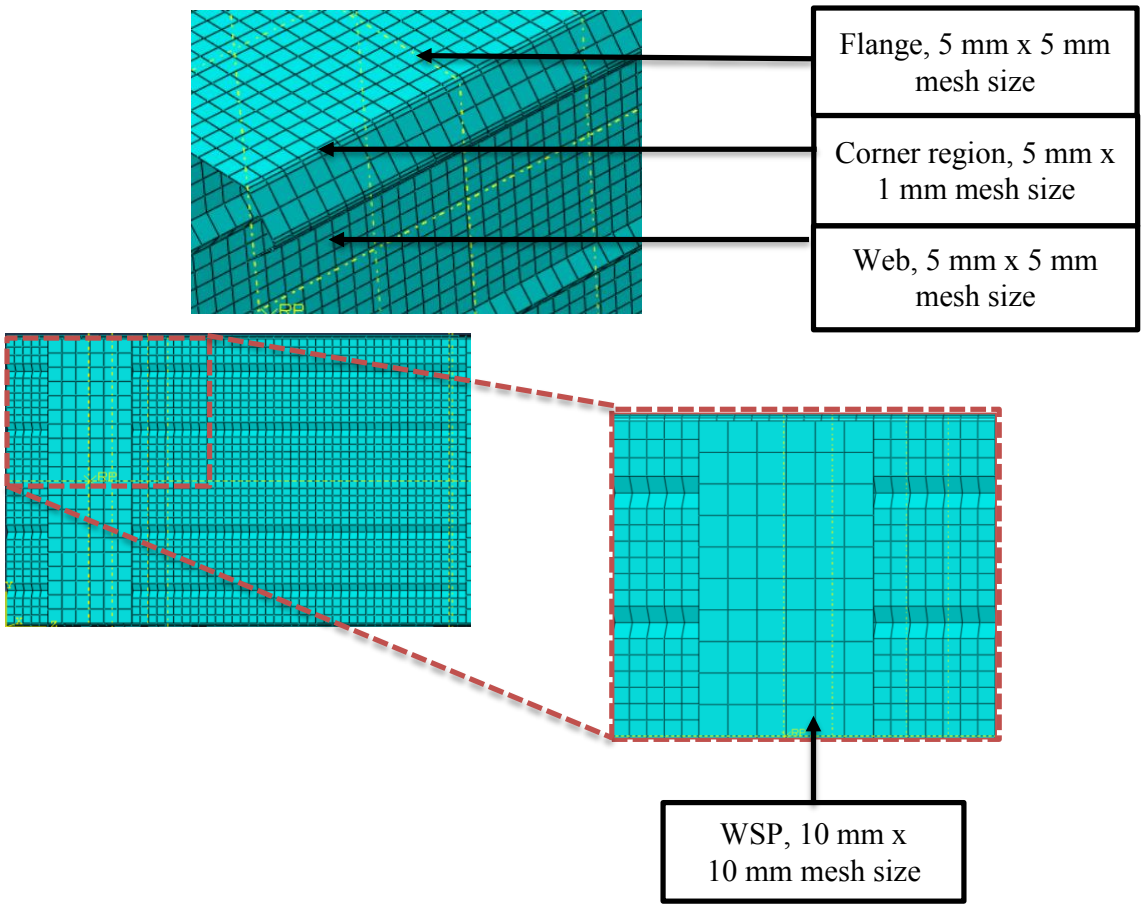

Fig. 4: Mesh refinement of SupaCee section and WSP

2.3 Material Properties

Engineering stress-strain behaviour of steel which was used in the modelling process is illustrated by Fig. 5. Strain hardening is negligible considering the CFS stress-strain behaviour, as Haidarali and Nethercot [21] proved that the structural behaviour of CFS was not influenced by the strain hardening. On that account, bilinear model was preferred to state the stress-strain behaviour of CFS in the numerical modelling. Considering the recent past research studies [22-24], which investigated the behaviour of CFS sections, an elastic-perfectly plastic material was chosen with nominal yield strength to model SupaCee section. Material properties such as

elastic modulus and Poisson's ratio were assigned with value of 200 GPa and 0.3, respectively. Moreover, density of steel was selected as 7850 kg/m^3. Corner strength enhancement and residual stress were not considered as the corner strength enhancement did not cause a major difference in the results as reported by Wang and Young [25] and Schafer et al. [26]. Moreover, Schafer et al. [26] stated that both residual stress and corner strength enhancement effects can be neglected assuming that they offset each other.

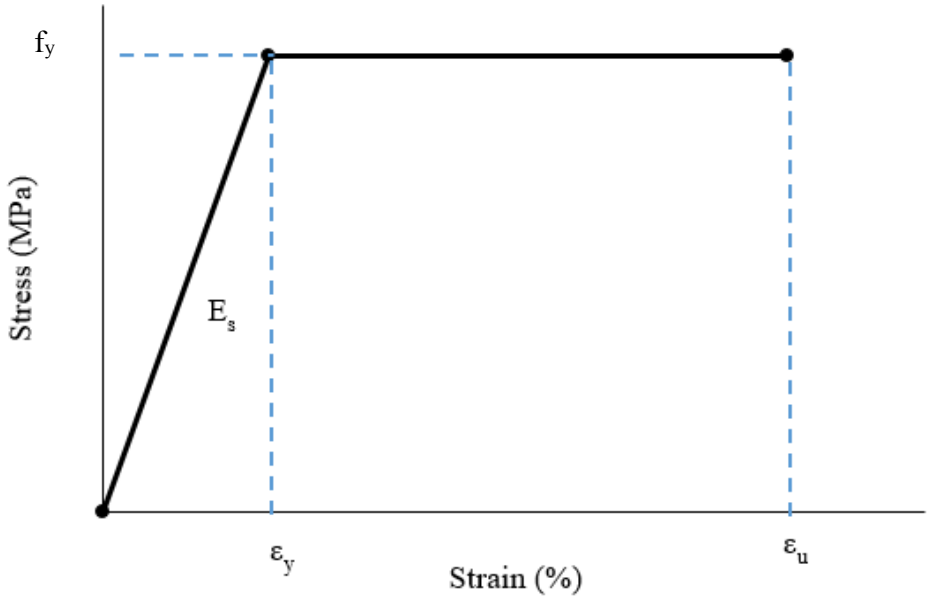

Fig. 5. Engineering stress-strain curve for the CFS applied in modelling

2.4 Boundary and Loading conditions

Reference points should be assigned to replicate the actual rigid elements and assign boundary conditions of the support and loading points. Thus, boundary conditions of simply supported: pin and roller support context, assigned to the reference points. To simulate the loading condition, vertically downward displacement was assigned in the reference point. Moreover, lateral restraints were applied in both flanges of the beam. Reference point, assignment of boundary conditions and loading pattern are illustrated in Fig.6 and Table 1.

The effect of not using the angle straps adjacent to loading and support points on the shear capacity was taken into consideration by Keerthan and Mahendran [27]. Accordingly, shear capacity reduction up to 10% was observed without the utilization of straps. Based on the results obtained by Keerthan and Mahendran [27] straps were included in this study adjacent to support and loading points to eliminate unbalanced shear flow as well as flange distortion.

Hence, effect of boundary conditions on shear capacity of SupaCee sections with web openings could be neglected

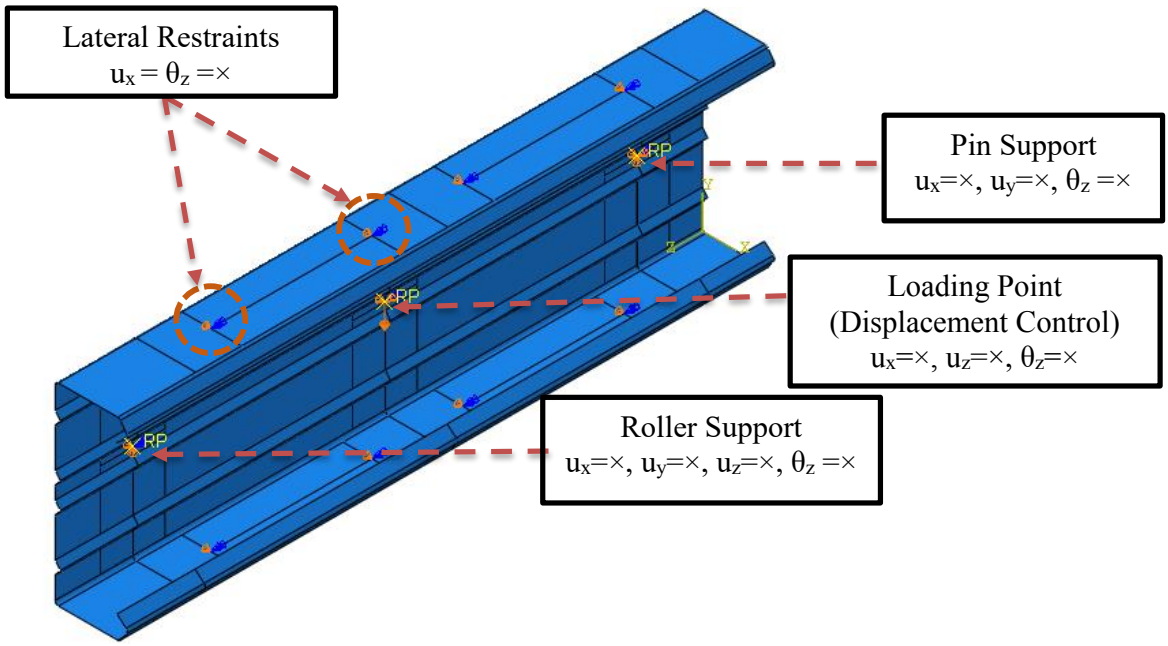

Fig. 6: Boundary and Loading conditions

Table 1. Boundary Conditions of Finite Element Model

Boundary conditions	Left Support	Right Support	Loading point	Lateral Restraints
u_x	×	×	×	×
u_y	×	×	0	0
u_z	×	0	×	0
θ_x	0	0	0	0
θ_y	0	0	0	0
θ_z	×	×	×	×
Note: 0 - free, × - restrained, u- displacement, θ- rotational movement				

2.5 Geometrical Imperfection

Structural defects of the SupaCee section were considered in this study in the form of adding geometrical imperfection to the section while performing the non-linear analysis. Imperfections are usually added to the geometry of CFS sections by perturbations in the nonlinear analysis. In ABAQUS [19], there are three methods to add initial geometrical imperfections in the perfect model to replicate the actual deformations in the elements: Based on the linear superposition

of buckling eigen modes geometric imperfection can be added, direct entry of imperfection and node number in the data lines and defining the displacement in the initial *STATIC analysis [28-29]. The first method was considered in this study and initial elastic buckling analysis was performed to obtain the critical buckling modes [15]. Lowest eigen value buckling modes were considered as the critical buckling modes. From the buckling analysis and based on the critical buckling modes, geometric imperfection with the magnitude of 0.64*t [15], where t is thickness of the section, was added by using the keyword of "*IMPERFECTION" in ABAQUS. Selection of geometrical imperfection for the analysis was based on the past study on shear performance of SupaCee sections conducted by Pham and Hancock [15] and the validation process of this study. Hence, the results obtained from this study accommodates possible structural and geometrical defects of the section.

2.6 Solution control parameters

Numerical analysis of thin sections should consider two significant factors: convergence and integration accuracy. As stated in the overview section, linear elastic buckling analysis and nonlinear analysis were proceeded in order to obtain shear capacity of the section. The former, carried out to obtain critical buckling mode and to add the geometric imperfection. Whereas, the latter performed to find the shear capacity as well as failure mechanisms using the static Riks method, similarly to the literature [30-36].

2.7 Validation of Finite Element Model

Verification of modelling properties against experimental investigations is necessary to ensure the reliability of the parametric study results. Appropriate existing experiments regarding the shear behaviour of SupaCee sections were selected for the validation process. Pham and Hancock [15] experimented SupaCee sections with the depth of 150 mm and 200 mm and three different thicknesses (1.2 mm, 1.5 mm and 2.4 mm) were considered. Six results of the experiment were selected for validation process and same number of FE models were generated replicating actual boundary conditions, material characteristics, element types and loading patterns. Results obtained from FE analysis were compared with experiment results and Table 2 shows the comparison of the outcomes of Finite Element Analysis (FEA) and experiments.

219 Table 2. Comparison of FEA and Experimental values

Section	d	t	f_y	Experiment results (Pham and Hancock [15])	FEA values	Experiment/FEA
	(mm)	(mm)	(MPa)	(kN)	(kN)	
SC15012	150	1.2	589.71	42.13	45.72	0.92
SC15015	150	1.5	533.88	55.58	58.75	0.95
SC15024	150	2.4	513.68	97.99	94.79	1.03
SC20012	200	1.2	593.30	46.48	49.64	0.94
SC20015	200	1.5	532.03	62.07	62.86	0.99
SC20024	200	2.4	504.99	124.21	111.70	1.11
Mean						0.99
COV						0.07
Note: d - total sectional depth, t - thickness of section f_y - yield strength of material						

220 Ultimate shear capacities derived from FE models displayed exemplary concurrence with
221 experimental outcomes with mean value of 0.99 and COV value (Coefficient of Variation) of
222 0.07. In addition, the load vs deflection curve for the experiment study and the FE model was
223 compared in Fig. 7 and it demonstrates good agreement. Discrepancy in the illustrated
224 comparison is due to initial slip in experiments which was not incorporated in numerical
225 studies. Considering the aforementioned comparisons, the developed FE model was selected to
226 analyse the shear behaviour of SupaCee sections without openings. Failure pattern of
227 experimental section and numerical model showed similar illustration as well. Failure modes
228 of both experiment and numerical studies is compared in Fig. 8.

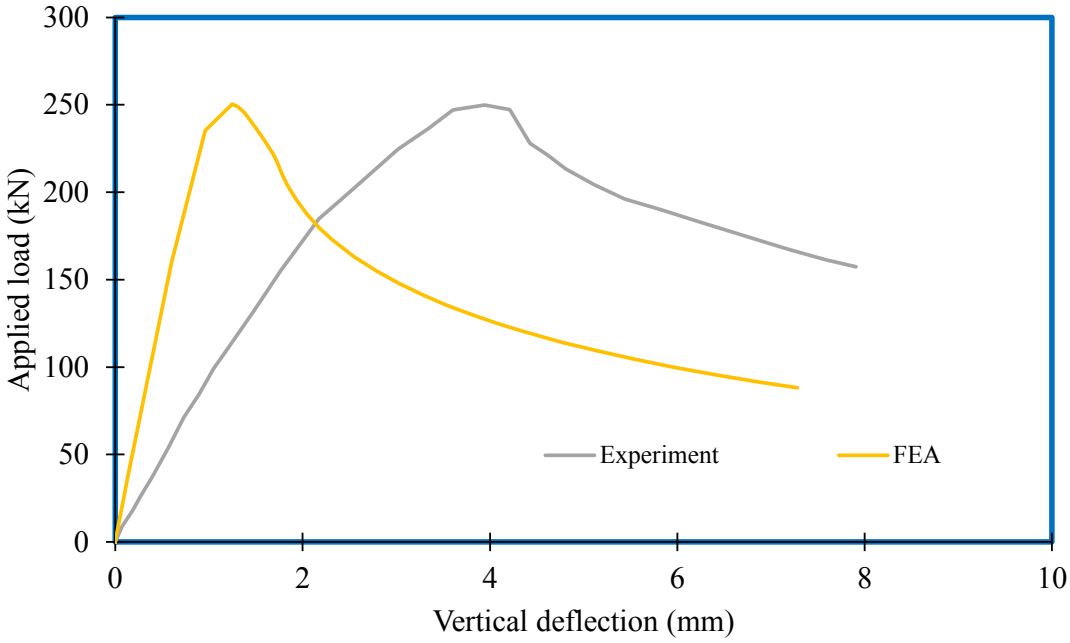

Fig. 7: Comparison of Applied load vs deflection curve for section SC20015 [15]

229

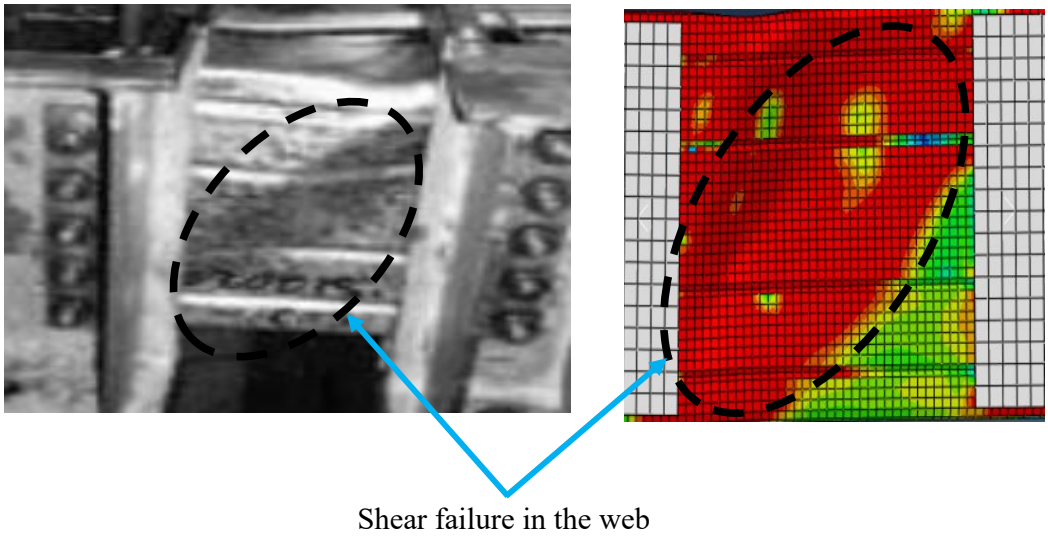

Fig. 8: Comparison of failure pattern of SupaCee section (FEA vs Experiment) for section SC20015 [15]

230

231 The validation process was also carried out for LCB (Lipped Channel Beam) sections with web
232 openings to ensure the parametric model characteristics, boundary conditions and failure
233 pattern with web openings. Keerthan and Mahendran [37] studied the shear behaviour of LCB
234 sections with web openings. The results were obtained from comprehensive experiments
235 completed by Keerthan and Mahendran [37] and developed models were validated with the
236 experiment outcomes. Five LCB sections with various web opening sizes were selected for the

237 validation process. Details of the selected sections and the results of the validation process are
238 detailed in the Table 3.

239 Table 3. Comparison of FEA and Experiment values of LCB sections with openings [37]

Section (d x b_f x b_l x t)	f_y (MPa)	d_{wh} (mm)	Experiment (kN) [37]	FE (kN)	Experiment/FE
160 x 65 x 15 x 1.9	515	0	73.80	78.67	0.94
160 x 65 x 15 x 1.9	515	30	65.37	68.53	0.95
160 x 65 x 15 x 1.9	515	60	49.53	54.09	0.92
160 x 65 x 15 x 1.9	515	100	27.61	29.25	0.94
160 x 65 x 15 x 1.9	515	125	16.88	15.68	1.08
Mean					0.97
COV					0.07
Note: d - section depth, b_f - flange width, b_l - flange depth, t - thickness of section f_y - yield strength and d_{wh} - web opening diameter					

240 Validation results exhibit good agreement with experiment results with mean value of 0.97 and
241 COV value of 0.07. Moreover, Fig. 9 illustrates failure mode of the section, which is more
242 evident for the acceptance of developed model to carryout parametric studies.

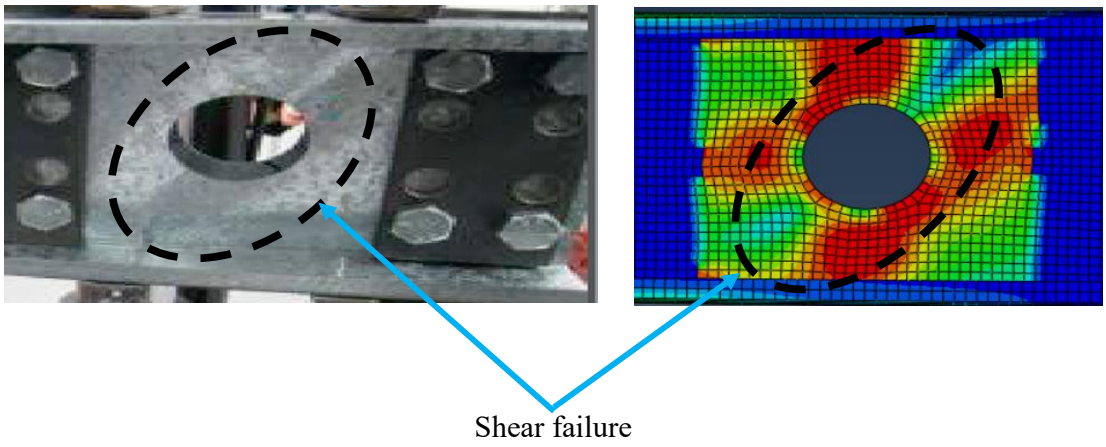

243 Fig. 9: Failure mode comparison of LCB section (160x65x15x1.9) with web opening (60 mm) [37]

244 Based on both validation results and other comparisons in terms of failure patterns and applied
245 load vs deflection graphs, numerical models were created to obtain ultimate shear capacity of
246 SupaCee sections with web openings and without web openings.

3 Parametric study

Parametric plan was developed to analyse the shear behaviour of SupaCee sections with web openings after the comprehensive validation process. Three different sections with the depth (H) of 150 mm, 200 mm and 250 mm were proposed to be analysed in detail with thicknesses (t) of 1 mm, 2 mm and 2.5 mm. Dimension details are illustrated in the Fig. 10 and mentioned in the Table 3. Moreover, three material yield strengths (f_y) (300MPa, 450MPa and 600MPa) were selected whereas web opening ratios (d_{wh}/d_1) were chosen as 0, 0.2, 0.4, 0.6, 0.7 and 0.8. Previous investigations [28, 38-39] with web openings were taken into consideration for the selection of web opening ratios to avoid the failure due to Vierendeel mechanism, which leads to additional shear strength generation. Hence, the web opening ratio was limited to 0.8. In addition, the aspect ratio was chosen as 1.0 to ensure the failure is predominantly by shear. All aforementioned parameters were considered for the parametric analysis. Overall, 162 FE models were developed to obtain ultimate shear capacities of SupaCee sections with web openings. Table 4 illustrates parametric plan of intended FEA.

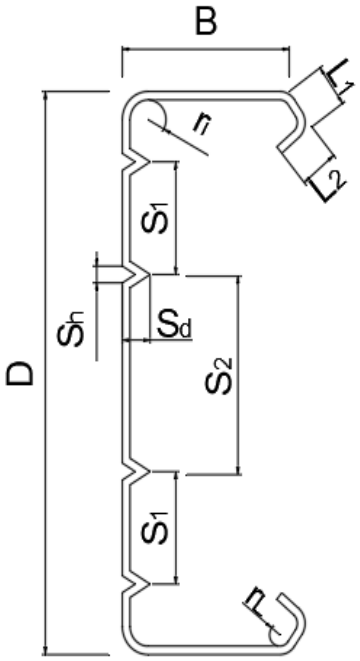

Fig. 10: Illustration of SupaCee section profile

Table 3. Dimension details of selected SupaCee sections

H (mm)	B (mm)	L_1 (mm)	L_2 (mm)	a_1 (mm)	a_2 (mm)	S_1 (mm)	S_2 (mm)	S_h (mm)	S_d (mm)	r_i (mm)	r_L (mm)
150	50	12	12	125	95	40	20	10	5	2	2
200	65	15	15	125	95	40	70	10	5	2	2
250	75	15	15	125	95	40	120	10	5	2	2

Table 4. Parametric plan of intended investigation

Section	Thickness	web hole diameter ratio	Strength	No. of Models
H x B (mm x mm)	t (mm)	d_{wh}/d_1	f_y (MPa)	
150 x 50	1, 2, 2.5	0, 0.2, 0.4, 0.6, 0.7, 0.8	300, 450, 600	54
200 x 65	1, 2, 2.5	0, 0.2, 0.4, 0.6, 0.7, 0.8	300, 450, 600	54
250 x 75	1, 2, 2.5	0, 0.2, 0.4, 0.6, 0.7, 0.8	300, 450, 600	54
Total				162

Tables 5-7 summarise the obtained parametric study results for sections of 150 mm, 200 mm and 250 mm, respectively. Results include ultimate shear capacity (V_{nl}) of the sections and the shear reduction factor (q_s) for each web-opening ratio (d_{wh}/d_1) with corresponding yield strengths (f_y) and thicknesses (t). Fig. 11 illustrates the failure modes of SupaCee section (150x50x1) with web opening of 0.2 ($d_{wh}/d_1 = 0.2$) and shear failure pattern of the SupaCee section.

Table 5. Parametric study results of section 150x50

H (mm)	t (mm)	d_{wh}/d_1	f_y = 300 MPa		f_y = 450 MPa		f_y = 600 MPa	
			V_{nl}	q_s	V_{nl}	q_s	V_{nl}	q_s
150	1	0	20.38	1.00	29.42	1.00	36.84	1.00
150	1	0.2	17.40	0.85	24.29	0.83	30.32	0.82
150	1	0.4	13.77	0.68	19.56	0.67	24.31	0.66
150	1	0.6	9.39	0.46	13.18	0.45	16.73	0.45
150	1	0.7	6.39	0.31	9.17	0.31	11.77	0.32
150	1	0.8	4.37	0.21	6.22	0.21	7.91	0.21
150	2	0	44.27	1.00	64.84	1.00	84.81	1.00
150	2	0.2	40.57	0.92	59.11	0.91	76.23	0.90
150	2	0.4	30.83	0.70	44.02	0.68	56.80	0.67
150	2	0.6	21.93	0.50	31.58	0.49	40.58	0.48
150	2	0.7	15.59	0.35	22.33	0.34	28.85	0.34
150	2	0.8	10.92	0.25	15.62	0.24	20.11	0.24

150	2.5	0	56.31	1.00	82.38	1.00	108.05	1.00
150	2.5	0.2	50.88	0.90	74.47	0.90	96.90	0.90
150	2.5	0.4	40.68	0.72	58.11	0.71	74.87	0.69
150	2.5	0.6	27.59	0.49	39.56	0.48	50.92	0.47
150	2.5	0.7	20.81	0.37	29.73	0.36	38.24	0.35
150	2.5	0.8	15.03	0.27	21.39	0.26	27.29	0.25

271 Table 6. Parametric study results of section 200x65

H (mm)	t (mm)	d_{wh}/d_1	f_y=300 MPa		f_y=450 MPa		f_y=600 MPa	
			V_{nl}	q_s	V_{nl}	q_s	V_{nl}	q_s
200	1	0	25.55	1.00	31.46	1.00	37.31	1.00
200	1	0.2	22.88	0.90	29.90	0.95	35.53	0.95
200	1	0.4	16.38	0.64	21.84	0.69	26.10	0.70
200	1	0.6	10.92	0.43	14.81	0.47	18.03	0.48
200	1	0.7	8.21	0.32	11.43	0.36	14.34	0.38
200	1	0.8	5.27	0.21	7.40	0.24	9.36	0.25
200	2	0	57.29	1.00	83.05	1.00	102.25	1.00
200	2	0.2	54.77	0.96	75.72	0.91	92.80	0.91
200	2	0.4	38.74	0.68	54.54	0.66	68.28	0.67
200	2	0.6	24.96	0.44	35.05	0.42	43.80	0.43
200	2	0.7	19.57	0.34	27.71	0.33	34.72	0.34
200	2	0.8	12.98	0.23	18.59	0.22	23.78	0.23
200	2.5	0	72.77	1.00	106.97	1.00	139.48	1.00
200	2.5	0.2	69.07	0.95	99.07	0.93	128.48	0.92
200	2.5	0.4	49.56	0.68	71.24	0.67	91.57	0.66
200	2.5	0.6	32.96	0.45	46.72	0.44	58.80	0.42
200	2.5	0.7	26.42	0.36	37.39	0.35	47.03	0.34
200	2.5	0.8	18.05	0.25	25.58	0.24	32.90	0.24

272 Table 7. Parametric study results of section 250x75

H (mm)	t (mm)	d_{wh}/d_1	f_y=300 MPa		f_y=450 MPa		f_y=600 MPa	
			V_{nl}	q_s	V_{nl}	q_s	V_{nl}	q_s
250	1	0	27.19	1.00	32.82	1.00	38.88	1.00
250	1	0.2	23.72	0.87	30.57	0.93	36.88	0.95
250	1	0.4	18.68	0.69	24.18	0.74	29.00	0.75
250	1	0.6	11.50	0.42	15.29	0.47	18.64	0.48
250	1	0.7	8.89	0.33	11.67	0.36	14.54	0.37
250	1	0.8	5.94	0.22	7.93	0.24	9.76	0.25
250	2	0	67.29	1.00	90.91	1.00	112.34	1.00
250	2	0.2	58.05	0.86	80.40	0.88	100.61	0.90
250	2	0.4	43.13	0.64	59.55	0.66	74.15	0.66
250	2	0.6	28.89	0.43	39.42	0.43	49.87	0.44
250	2	0.7	21.97	0.33	29.39	0.32	35.84	0.32
250	2	0.8	15.49	0.23	21.90	0.24	26.62	0.24

250	2.5	0	87.52	1.00	124.97	1.00	153.72	1.00
250	2.5	0.2	78.56	0.90	110.57	0.88	138.59	0.90
250	2.5	0.4	61.49	0.70	82.79	0.66	102.87	0.67
250	2.5	0.6	39.41	0.45	55.37	0.44	69.43	0.45
250	2.5	0.7	29.44	0.34	40.27	0.32	49.03	0.32
250	2.5	0.8	20.46	0.23	28.73	0.23	35.65	0.23

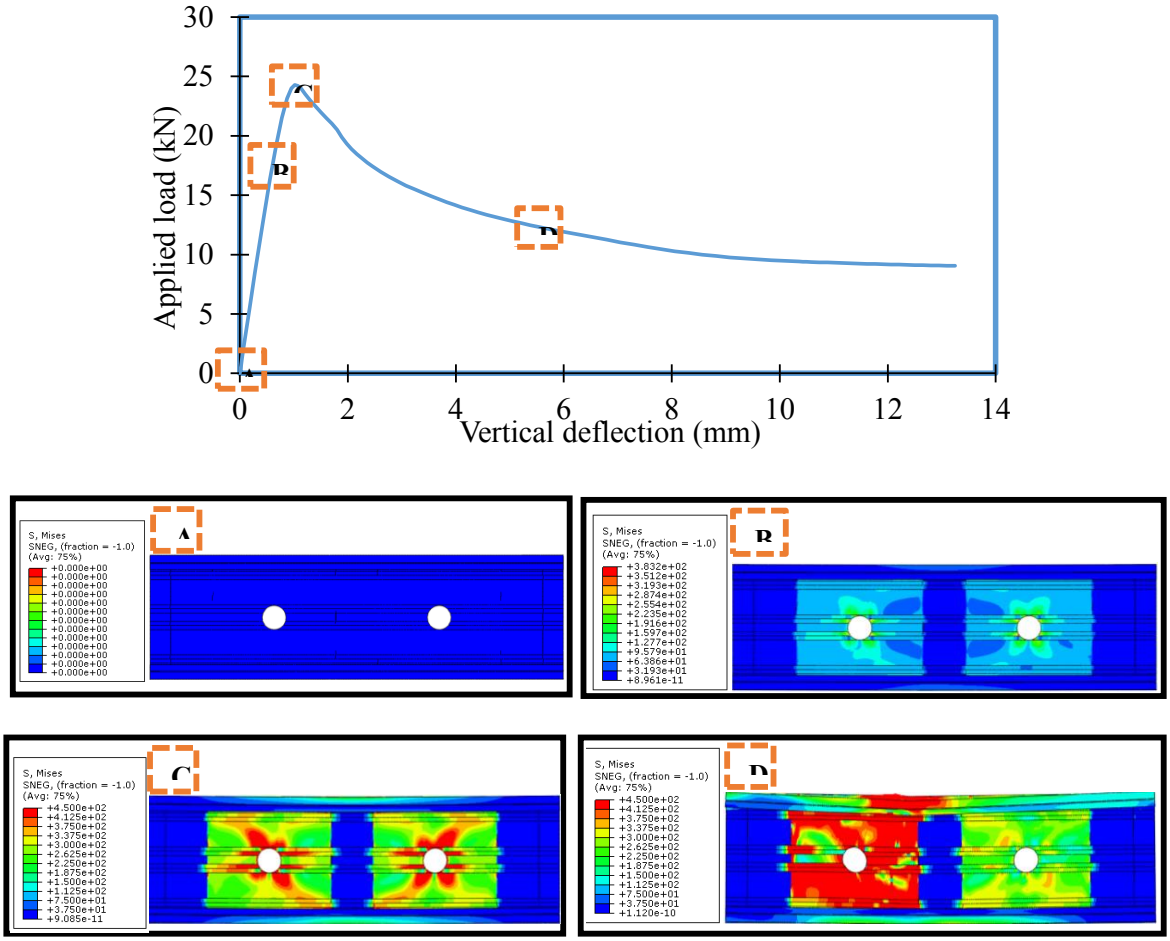

Fig. 11: Failure modes of section 150x50x1 with web opening ratio of 0.6

Figs. 12 - 13 compare the effect of web opening ratio in the shear capacity of the section 200x65x2 with a yield strength of 450 MPa. It clearly indicates that the increase in the web opening ratio affects the shear capacity of the section adversely. Reduction percentage for the shear capacity was observed as 8.84%, 34.33%, 57.80%, 66.64% and 77.62% for the web opening ratios of 0.2, 0.4, 0.6, 0.7 and 0.8, respectively, when compared to the solid section's (200x65x1 with yield strength of 450 MPa) shear capacity.

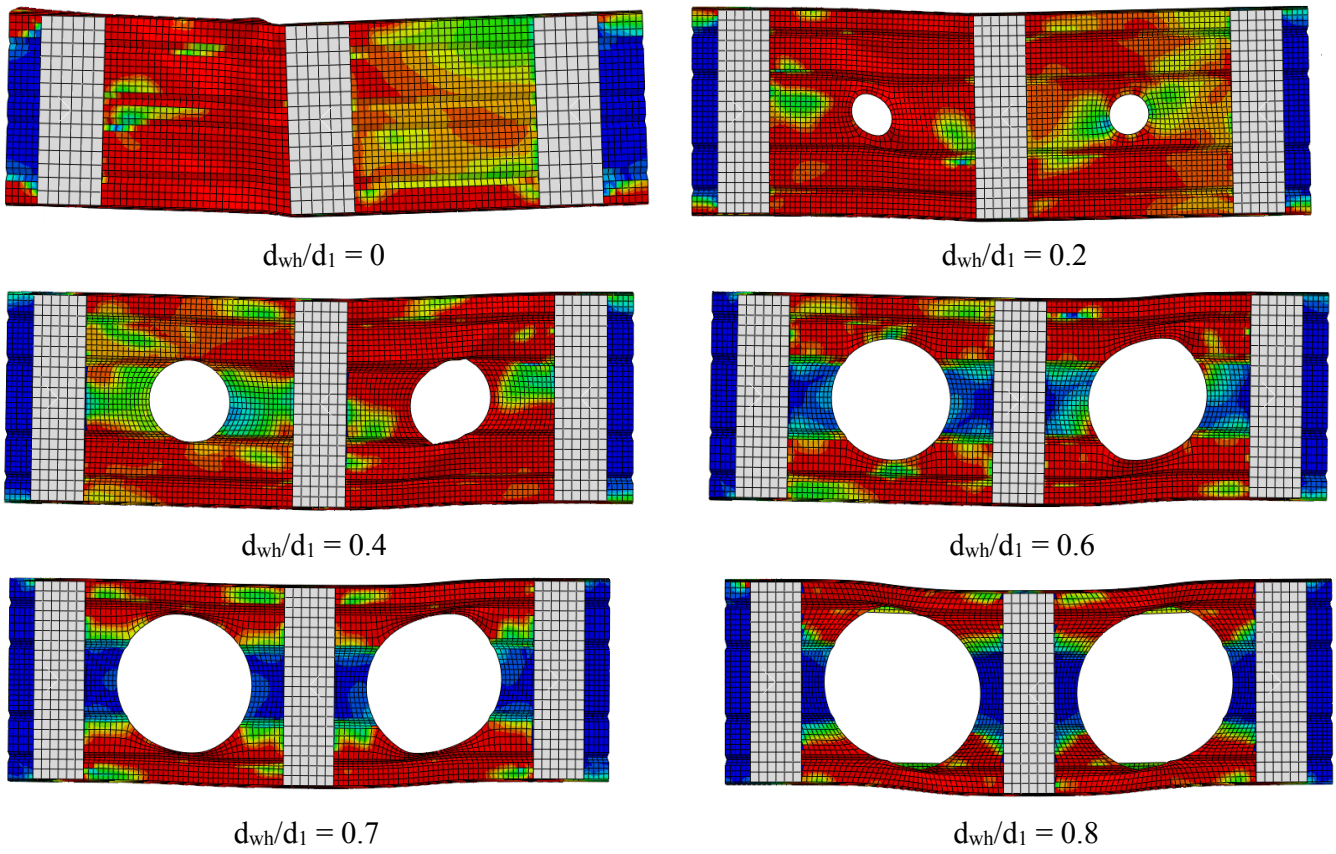

Fig. 12: Failure modes of section 200 with respect to web opening ratios

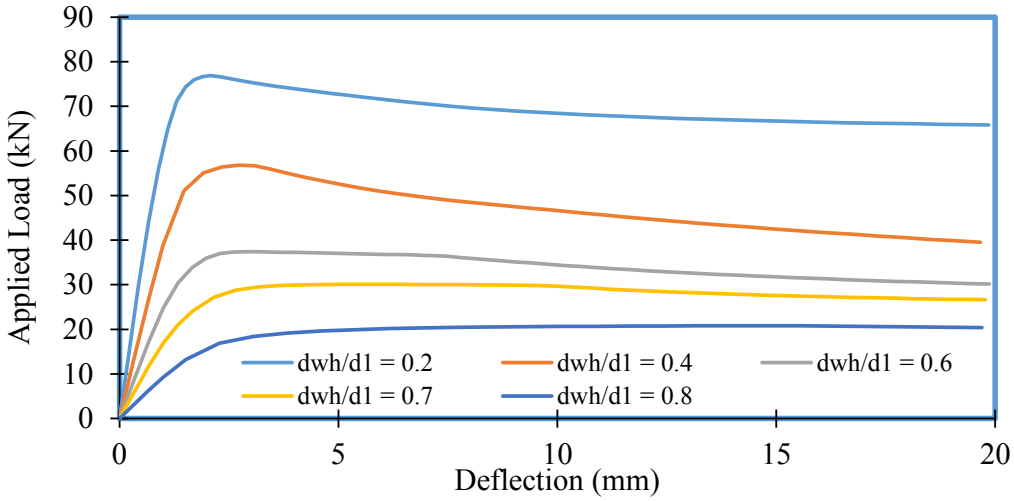

Fig. 13: Shear load vs Deflection graph with respect to web opening ratios

The shear capacity of a section also depends on the thickness and yield strength. Both parameters have a positive impact on the shear capacity of SupaCee sections, which is

illustrated in Fig. 14 and Fig. 15. Table 8 compares the effect of thickness and yield strength in the shear capacity of SupaCee section, with respect to web opening size in terms of percentage.

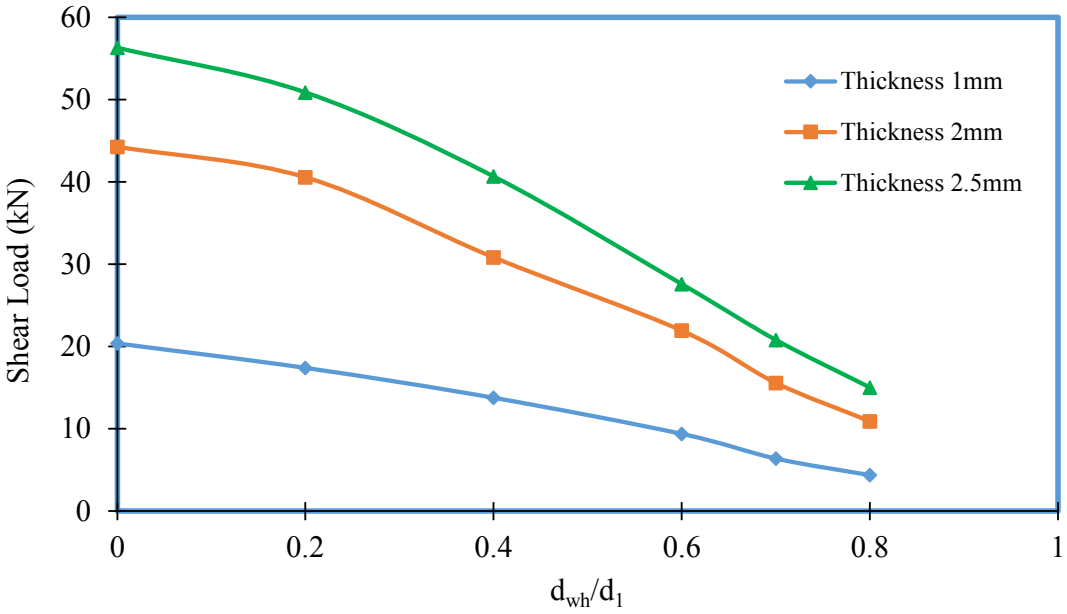

Fig. 14: Shear load comparison with respect to thickness for section (300 MPa) 150x50

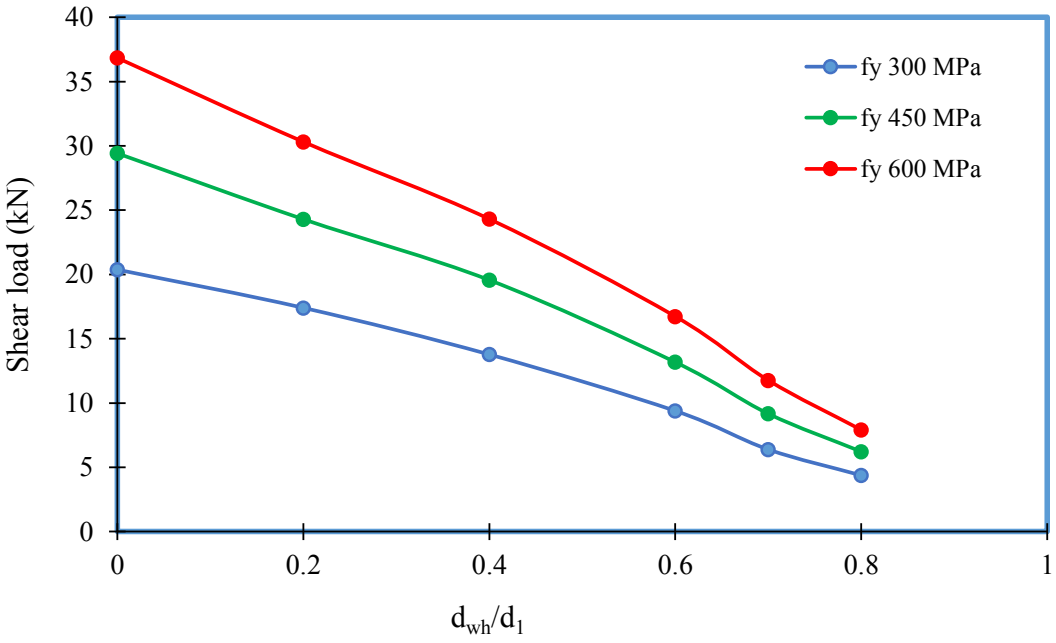

Fig. 15: Shear load comparison with respect to yield strength for section 150x50 with thickness of 1 mm

Table 8. Shear capacity reduction (%) comparison with respect to thickness and yield strength for section 150x50x1

Shear capacity reduction percentage (%)					
web opening ratio (fy = 300 MPa) / Thickness (mm)	0.2	0.4	0.6	0.7	0.8
1	14.59	32.39	53.93	68.64	78.54
2	8.38	30.36	50.46	64.79	75.34
2.5	9.64	27.76	51.01	63.05	73.31
web opening ratio / Yield strength (MPa)	0.2	0.4	0.6	0.7	0.8
300	14.59	32.39	53.93	68.64	78.54
450	17.42	33.5	55.21	68.84	78.87
600	17.71	34.02	54.58	68.06	78.53

4 Review of Shear design rules

Researchers have analysed the shear behaviour of various CFS sections, such as Lite Steel Beam (LSB) [40-43], Lipped Channel Beam (LCB) [37-38] and Hollow Flange Channel Beams (HFCB) [24]. In addition, Pham and Hancock [15] investigated the shear behaviour of SupaCee sections. Hence, this section reviews the current design equations and rules to predict the shear capacity of LCB sections and SupaCee sections.

Pham and Hancock [44-45] carried out experimental and numerical work to understand the shear behaviour of LCB sections. Two separate depths and three various thicknesses were considered and equations were proposed to predict the shear capacity of LCB sections (Eqs. (1) - (3)). Prediction of shear capacity using these equations includes available post buckling strength of LCB and possible fixity issue in the web-flange juncture.

$$V_v = \left[1 - 0.15\left(\frac{V_{cr}}{V_y}\right)^{0.4}\right]\left(\frac{V_{cr}}{V_y}\right)^{0.4} V_y \quad (1)$$

$$V_y = 0.6\, f_{yw} d_1 t_w \quad (2)$$

$$V_{cr} = \frac{k_v \pi^2 E t_w^{\,3}}{12(1-v^2)d_1} \quad (3)$$

Where, V_v= nominal shear capacity, V_y= shear yield capacity, V_{cr}= elastic shear buckling capacity, t_w= web thickness, d_1= clear height of the web, f_{yw}= web yield stress, E= modulus of elasticity and k_v= elastic shear buckling coefficient of LCB.

Keerthan and Mahendran [40-41] studied the shear capacity of LSB sections and proposed new design equations. The equations included the available post buckling strength and additional fixity in the web-flange juncture (Eqs. (4) – (6)). On that note, shear-buckling coefficient (k_{LCB}) (Eqs. (7) – (11)) were proposed by Keerthan and Mahendran [46] to accommodate additional fixity in the web-flange juncture in LCB sections.

$$V_v = V_y = 0.6\, f_{yw} d_1 t_w \quad \text{for} \quad \frac{d_1}{t_w} \le \sqrt{\frac{Ek_v}{f_{yw}}} \tag{4}$$

(Shear yielding capacity)

$$V_v = 0.6 t_w^2 \sqrt{E k_v f_{yw}} \quad \text{for} \quad \sqrt{\frac{Ek_v}{f_{yw}}} < \frac{d_1}{t_w} \le 1.508 \sqrt{\frac{Ek_v}{f_{yw}}} \tag{5}$$

(Inelastic shear buckling capacity)

$$V_v = V_{cr} = \frac{k_v \pi^2 E t_w^3}{12(1-v^2) d_1} \quad \text{for} \quad \frac{d_1}{t_w} > 1.508 \sqrt{\frac{Ek_v}{f_{yw}}} \tag{6}$$

(Elastic shear buckling capacity)

$$k = k_{ss} + 0.23(k_{sf} - k_{ss}) \tag{7}$$

$$k_{ss} = 5.34 + \frac{4}{(a/d_1)^2} \text{ for } \frac{a}{d_1} \ge 1 \tag{8}$$

$$k_{ss} = 4 + \frac{5.34}{(a/d_1)^2} \text{ for } \frac{a}{d_1} < 1 \tag{9}$$

$$k_{sf} = 8.98 + \frac{5.61}{(a/d_1)^2} - \frac{1.99}{(a/d_1)^3} \text{ for } \frac{a}{d_1} \ge 1 \tag{10}$$

$$k_{sf} = \frac{5.34}{(a/d_1)^2} + \frac{2.31}{(a/d_1)} - 3.44 + \frac{8.39}{(a/d_1)} \text{ for } \frac{a}{d_1} < 1 \tag{11}$$

Where k_{ss} and k_{sf} are the shear buckling coefficients of plates with simple-simple and simple-fixed boundary conditions, a, is the shear span of web, d_1 is the clear height of web and f_{yw} is the web yield stress.

Design equations based on Direct Strength Method (DSM) to predict the shear load was reported by Keerthan and Mahendran [46]. Eqs. (12) – (14) only considered two regions among elastic shear buckling, shear yielding and inelastic shear buckling, which was adequate with respect to DSM format. Particular approach was followed by Pham and Hancock [44-45] earlier.

$$\frac{V_v}{V_y} = 1 \text{ for } \lambda \leq 0.815 \tag{12}$$

$$\frac{V_v}{V_y} = \left[1 - 0.15\left(\frac{1}{\lambda^2}\right)^{0.55}\right]\left(\frac{1}{\lambda^2}\right)^{0.55} \text{ for } \lambda > 0.815 \tag{13}$$

$$Where,\ \lambda = \sqrt{\frac{V_y}{V_{cr}}} \tag{14}$$

The reduction factor (q_s): the ratio of the nominal shear strength with openings (V_{nl}) to the shear strength of the LCBs without web openings (V_v) is commonly used to determine the shear strength of LCB sections with web openings. Equations proposed by Shan et al. [47] (Eqs. (15) – (17)) also recommended a reduction factor to predict the shear capacity of LCB sections with web openings. Moreover, it was stated that web opening ratio is the influencing factor of shear capacity (V_{nl}) of LCB sections with web openings and ratio of clear web height to web thickness was not an influencing factor.

$$\mathrm{V_{nl}} = \mathrm{q_s V_v} \tag{15}$$

$$\mathrm{q_s} = -3.66\frac{\mathrm{d_{wh}}}{\mathrm{d_1}} + 1.71 \qquad \text{for} \quad \frac{d_{wh}}{d_1} \leq 0.38 \tag{16}$$

$$\mathrm{q_s} = -0.38\frac{d_{wh}}{d_1} + 0.46 \qquad \text{for} \quad 0.38 < \frac{\mathrm{d_{wh}}}{\mathrm{d_1}} \leq 1.0 \tag{17}$$

Where d_{wh} – depth of web openings, d_1 – clear height of web.

Eiler et al. [48] also studied the shear behaviour of LCB sections with web openings and proposed design equations based on the reduction factor. Proposed equations (Eqs. (18) – (21)) have been included in AS/NZS 4600 [16] and AISI S100 [17].

$$q_s = 1 \quad \text{for} \quad \frac{c}{t} \geq 54 \tag{18}$$

$$q_s = \frac{c}{54t} \quad \text{for} \quad 5 \leq \frac{c}{t} < 54 \tag{19}$$

$$c = \frac{d_1}{2} - \frac{d_{wh}}{2.83} \quad \text{for circular web openings} \tag{20}$$

$$c = \frac{d_1}{2} - \frac{d_{wh}}{2} \quad \text{for non-circular web openings} \tag{21}$$

Where, $\frac{d_{wh}}{d_1} < 0.7$, $\frac{d_{wh}}{t_w} \leq 200$, $15\text{mm} < d_{wh} \leq 150\text{mm}$, d_1 - depth of the web, d_{wh} - depth of web openings, t_w- web thickness and t - thickness of the section

Later, Keerthan and Mahendran [42-43] proposed equations (Eqs. (22) – (25)) for the shear capacity of LSB sections with web openings based on the shear capacity reduction factor applied to the shear capacity of the section without web openings. Meanwhile, Wanniarachchi et al. [38] studied the shear performance of LCB sections with non-circular web openings and proposed design equations based on area reduction method.

$$V_{nl} = q_s V_v \quad \text{for} \quad \frac{d_{wh}}{d_1} \leq 0.85 \tag{22}$$

$$q_s = 1 - 0.6\frac{d_{wh}}{d_1} \quad \text{for} \quad 0 < \frac{d_{wh}}{d_1} \leq 0.3 \tag{23}$$

$$q_s = 1.215 - 1.316\frac{d_{wh}}{d_1} \quad \text{for} \quad 0.3 < \frac{d_{wh}}{d_1} \leq 0.7 \tag{24}$$

$$q_s = 0.732 - 0.625\frac{d_{wh}}{d_1} \quad \text{for} \quad 0.7 < \frac{d_{wh}}{d_1} \leq 0.85 \tag{25}$$

Pham and Hancock [49] performed experiments and numerical analyses on SupaCee sections for their shear behaviour. Two different depths and three various thicknesses were selected for experiment procedure. Equations to predict the ultimate shear capacity of SupaCee sections were proposed based on AS/NZS 4600 [16] without Tension Field Action (TFA) (Eqs. (26) – (28)), AS 4100 [50] accounting TFA and DSM proposals with TFA (Eq. 29) and without TFA (Eqs. (30) – (32)).

$$V_v = 0.64\, f_y d_1 t_w \quad \text{for} \quad \frac{d_1}{t_w} \leq \sqrt{\frac{Ek_v}{f_y}} \tag{26}$$

$$V_v = 0.64 t_w^2 \sqrt{E k_v f_y} \quad \text{for} \quad \sqrt{\frac{Ek_v}{f_y}} < \frac{d_1}{t_w} \leq 1.415 \sqrt{\frac{Ek_v}{f_y}} \tag{27}$$

$$V_v = \frac{0.905 E k_v {t_w}^3}{d_1} \quad \text{for} \quad \frac{d_1}{t_w} > 1.415 \sqrt{\frac{Ek_v}{f_y}} \tag{28}$$

Where, k_v = shear buckling coefficient for the web panel only and $k_v = 5.34 + \frac{4}{(s/d1)^2}$ for unstiffened webs, d_1 = depth of the flat portion of the web measured along the plane of the web, t_w = thickness of web

$$V_v = \left[1 - 0.15 \left(\frac{V_{cr}}{V_y}\right)^{0.4}\right] \left(\frac{V_{cr}}{V_y}\right)^{0.4} V_y \tag{29}$$

$$V_v = V_y \quad \text{for} \quad \lambda_v \leq 0.815 \tag{30}$$

$$V_v = 0.815 \sqrt{V_{cr} V_y} \quad \text{for} \quad 0.815 < \lambda_v \leq 1.231 \tag{31}$$

$$V_v = V_{cr} \quad \text{for} \quad \lambda_v > 1.231 \tag{32}$$

Where, $\lambda_v = \sqrt{V_y / V_{cr}}$, $V_y = 0.6\, f_y d_1 t_w$, $V_{cr} = \frac{k_v \pi^2 E {t_w}^3}{12(1-v^2) d_1}$, k_v – Shear buckling coefficient for SupaCee section.

Since past studies and aforementioned investigations have not examined the shear behaviour of SupaCee sections with web openings, the intended numerical investigation focuses on the research gap in a detailed manner. Numerical investigation consists various differing parameters including web opening ratios (0, 0.2, 0.4, 0.6, 0.7 and 0.8).

5 Proposed shear design rules

Since experiments or numerical investigations in terms of shear behaviour of SupaCee sections with web openings were not conducted, new design provisions to predict the shear capacity of SupaCee sections with web circular web openings by using shear reduction factor is detailed in

354 this section. This approach was followed in the previous research [38, 42-43] and design codes
355 [16-17] to predict the shear capacity (V_{nl}) of section with openings by applying shear reduction
356 factor (q_s) to shear capacity of sections without web openings (V_v) based on depth ratio factor
357 (d_{wh}/d_1).

358 The shear reduction factor obtained from the numerical results of SupaCee sections with web
359 openings, were compared with the proposed shear reduction factors for LCB sections with web
360 openings as Keerthan and Mahendran [37], Shan et al. [47] and Eiler [48] proposed reduction
361 factors and shear equations for LCB sections and presented in Fig. 16. Equations proposed by
362 Eiler [48] were adopted in AISI S100. Also, Fig.17 compares prediction of previous studies for
363 a 150 mm section. The equations proposed for LCB sections in previous studies [37-38, 47-48]
364 and design standards [16-17] are not applicable for SupaCee sections. On the other hand, the
365 new design equations based on the reduction factor for SupaCee sections with web openings
366 are proposed (Eqs. (33) - (35)) and the proposed equations exhibit great agreement with the
367 numerical results as mean value is noted as 1.00 and COV value is 0.05. Comparison of
368 proposed reduction factor and reduction factor obtained from numerical results are stated in
369 Table 9 and Table 10. In addition, Fig. 18 explains the agreement of FE results with proposed
370 equation which matches well.

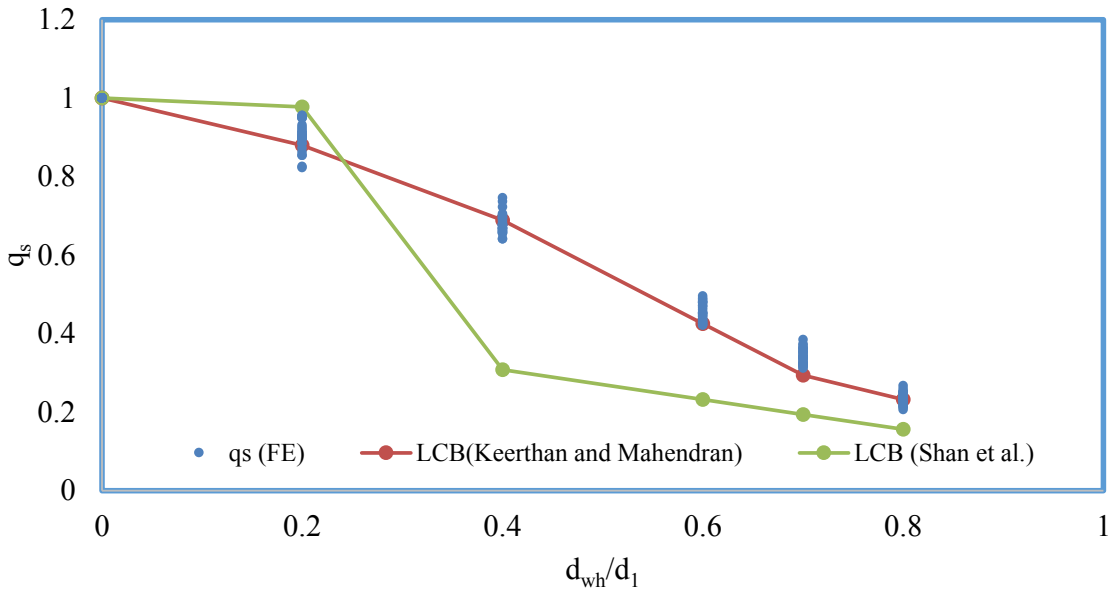

Fig. 16: Comparison of reduction factors with previous research studies on LCB sections with web openings [37, 47]

371

$$V_{nl} = q_s V_v \tag{33}$$

$$q_s = 1 - 0.71\left[\frac{d_{wh}}{d_1}\right] \qquad for\ 0 < \frac{d_{wh}}{d_1} \leq 0.4 \tag{34}$$

$$q_s = 1.10 - 1.08\left[\frac{d_{wh}}{d_1}\right] \qquad for\ 0.4 < \frac{d_{wh}}{d_1} \leq 0.8 \tag{35}$$

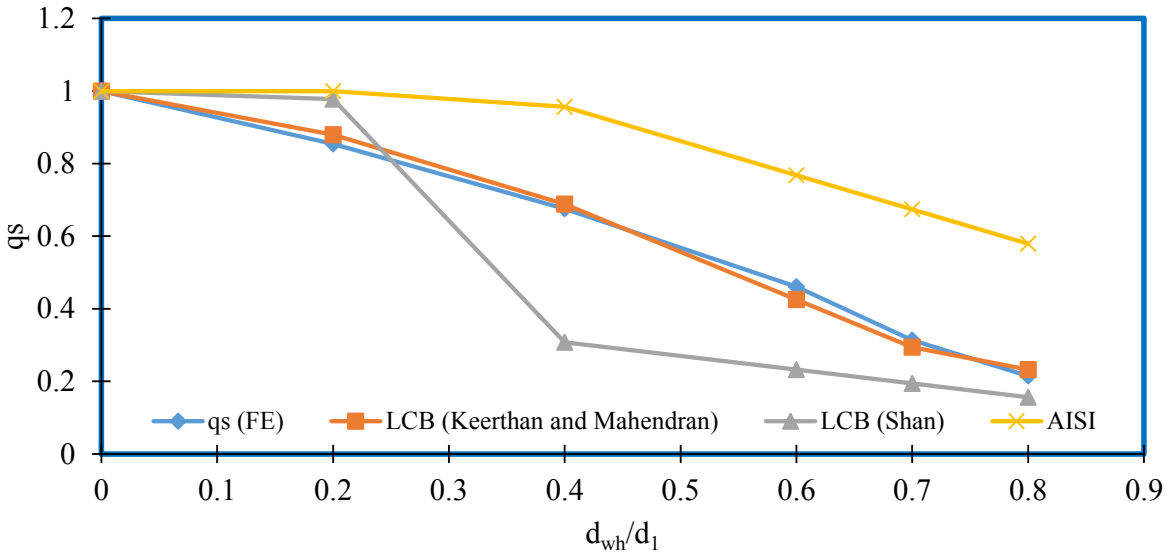

Fig. 17: Comparison of reduction factors with previous research studies on LCB sections with web openings for 150 section [17, 37, 47]

372

373 Table 9. Comparison of proposed reduction factor with obtained reduction factor from FE

374 results for $0 < \frac{d_{wh}}{d_1} \leq 0.4$

H (mm)	t (mm)	d_{wh}/d_1	strength (MPa)	FEA (without hole) (V_v)	FEA (with hole) (v_{nl})	Shear reduction factor q_s (FEA)	Proposed	FEA/ Proposed
150	1	0	300	20.38	20.38	1.00	1.00	1.00
150	1	0.2	300	20.38	17.40	0.85	0.86	0.99
150	1	0.4	300	20.38	13.77	0.68	0.72	0.94

150	2	0	300	44.27	44.27	1.00	1.00	1.00
150	2	0.2	300	44.27	40.57	0.92	0.86	1.07
150	2	0.4	300	44.27	30.83	0.70	0.72	0.97
150	2.5	0	300	56.31	56.31	1.00	1.00	1.00
150	2.5	0.2	300	56.31	50.88	0.90	0.86	1.05
150	2.5	0.4	300	56.31	40.68	0.72	0.72	1.01
150	1	0	450	29.42	29.42	1.00	1.00	1.00
150	1	0.2	450	29.42	24.29	0.83	0.86	0.96
150	1	0.4	450	29.42	19.56	0.67	0.72	0.93
150	2	0	450	64.84	64.84	1.00	1.00	1.00
150	2	0.2	450	64.84	59.11	0.91	0.86	1.06
150	2	0.4	450	64.84	44.02	0.68	0.72	0.95
150	2.5	0	450	82.38	82.38	1.00	1.00	1.00
150	2.5	0.2	450	82.38	74.47	0.90	0.86	1.05
150	2.5	0.4	450	82.38	58.11	0.71	0.72	0.98
150	1	0	600	36.84	36.84	1.00	1.00	1.00
150	1	0.2	600	36.84	30.32	0.82	0.86	0.96
150	1	0.4	600	36.84	24.31	0.66	0.72	0.92
150	2	0	600	84.81	84.81	1.00	1.00	1.00
150	2	0.2	600	84.81	76.23	0.90	0.86	1.05
150	2	0.4	600	84.81	56.80	0.67	0.72	0.93
150	2.5	0	600	108.05	108.05	1.00	1.00	1.00
150	2.5	0.2	600	108.05	96.90	0.90	0.86	1.04
150	2.5	0.4	600	108.05	74.87	0.69	0.72	0.97
200	1	0	300	25.55	25.55	1.00	1.00	1.00
200	1	0.2	300	25.55	22.88	0.90	0.86	1.04
200	1	0.4	300	25.55	16.38	0.64	0.72	0.89
200	2	0	300	57.29	57.29	1.00	1.00	1.00
200	2	0.2	300	57.29	54.77	0.96	0.86	1.11
200	2	0.4	300	57.29	38.74	0.68	0.72	0.94
200	2.5	0	300	72.77	72.77	1.00	1.00	1.00
200	2.5	0.2	300	72.77	69.07	0.95	0.86	1.11
200	2.5	0.4	300	72.77	49.56	0.68	0.72	0.95
200	1	0	450	31.46	31.46	1.00	1.00	1.00
200	1	0.2	450	31.46	29.90	0.95	0.86	1.11
200	1	0.4	450	31.46	21.84	0.69	0.72	0.97
200	2	0	450	83.05	83.05	1.00	1.00	1.00
200	2	0.2	450	83.05	75.72	0.91	0.86	1.06
200	2	0.4	450	83.05	54.54	0.66	0.72	0.92
200	2.5	0	450	106.97	106.97	1.00	1.00	1.00
200	2.5	0.2	450	106.97	99.07	0.93	0.86	1.08
200	2.5	0.4	450	106.97	71.24	0.67	0.72	0.93
200	1	0	600	37.31	37.31	1.00	1.00	1.00

200	1	0.2	600	37.31	35.53	0.95	0.86	1.11
200	1	0.4	600	37.31	26.10	0.70	0.72	0.98
200	2	0	600	102.25	102.25	1.00	1.00	1.00
200	2	0.2	600	102.25	92.80	0.91	0.86	1.06
200	2	0.4	600	102.25	68.28	0.67	0.72	0.93
200	2.5	0	600	139.48	139.48	1.00	1.00	1.00
200	2.5	0.2	600	139.48	128.48	0.92	0.86	1.07
200	2.5	0.4	600	139.48	91.57	0.66	0.72	0.92
250	1	0	300	27.19	27.19	1.00	1.00	1.00
250	1	0.2	300	27.19	23.72	0.87	0.86	1.02
250	1	0.4	300	27.19	18.68	0.69	0.72	0.96
250	2	0	300	67.29	67.29	1.00	1.00	1.00
250	2	0.2	300	67.29	58.05	0.86	0.86	1.00
250	2	0.4	300	67.29	43.13	0.64	0.72	0.89
250	2.5	0	300	87.52	87.52	1.00	1.00	1.00
250	2.5	0.2	300	87.52	78.56	0.90	0.86	1.05
250	2.5	0.4	300	87.52	61.49	0.70	0.72	0.98
250	1	0	450	32.82	32.82	1.00	1.00	1.00
250	1	0.2	450	32.82	30.57	0.93	0.86	1.08
250	1	0.4	450	32.82	24.18	0.74	0.72	1.03
250	2	0	450	90.91	90.91	1.00	1.00	1.00
250	2	0.2	450	90.91	80.40	0.88	0.86	1.03
250	2	0.4	450	90.91	59.55	0.66	0.72	0.91
250	2.5	0	450	124.97	124.97	1.00	1.00	1.00
250	2.5	0.2	450	124.97	110.57	0.88	0.86	1.03
250	2.5	0.4	450	124.97	82.79	0.66	0.72	0.92
250	1	0	600	38.88	38.88	1.00	1.00	1.00
250	1	0.2	600	38.88	36.88	0.95	0.86	1.10
250	1	0.4	600	38.88	29.00	0.75	0.72	1.04
250	2	0	600	112.34	112.34	1.00	1.00	1.00
250	2	0.2	600	112.34	100.61	0.90	0.86	1.04
250	2	0.4	600	112.34	74.15	0.66	0.72	0.92
250	2.5	0	600	153.72	153.72	1.00	1.00	1.00
250	2.5	0.2	600	153.72	138.59	0.90	0.86	1.05
250	2.5	0.4	600	153.72	102.87	0.67	0.72	0.93
Mean								1
COV								0.05

Table 10. Comparison of proposed reduction factor with obtained reduction factor from FE results for $0.4 < \frac{d_{wh}}{d_1} \leq 0.8$

H (mm)	t (mm)	d_{wh}/d_1	Strength (MPa)	FEA (without hole) (V_v)	FEA (with hole) (v_{nl})	Shear reduction factor q_s (FEA)	Proposed	FEA/Proposed
150	1	0.6	300	20.38	9.39	0.46	0.45	1.02
150	1	0.7	300	20.38	6.39	0.31	0.34	0.91
150	1	0.8	300	20.38	4.37	0.21	0.24	0.91
150	2	0.6	300	44.27	21.93	0.50	0.45	1.10
150	2	0.7	300	44.27	15.59	0.35	0.34	1.03
150	2	0.8	300	44.27	10.92	0.25	0.24	1.05
150	2.5	0.6	300	56.31	27.59	0.49	0.45	1.08
150	2.5	0.7	300	56.31	20.81	0.37	0.34	1.08
150	2.5	0.8	300	56.31	15.03	0.27	0.24	1.14
150	1	0.6	450	29.42	13.18	0.45	0.45	0.99
150	1	0.7	450	29.42	9.17	0.31	0.34	0.91
150	1	0.8	450	29.42	6.22	0.21	0.24	0.90
150	2	0.6	450	64.84	31.58	0.49	0.45	1.08
150	2	0.7	450	64.84	22.33	0.34	0.34	1.00
150	2	0.8	450	64.84	15.62	0.24	0.24	1.02
150	2.5	0.6	450	82.38	39.56	0.48	0.45	1.06
150	2.5	0.7	450	82.38	29.73	0.36	0.34	1.05
150	2.5	0.8	450	82.38	21.39	0.26	0.24	1.11
150	1	0.6	600	36.84	16.73	0.45	0.45	1.01
150	1	0.7	600	36.84	11.77	0.32	0.34	0.93
150	1	0.8	600	36.84	7.91	0.21	0.24	0.91
150	2	0.6	600	84.81	40.58	0.48	0.45	1.06
150	2	0.7	600	84.81	28.85	0.34	0.34	0.99
150	2	0.8	600	84.81	20.11	0.24	0.24	1.01
150	2.5	0.6	600	108.05	50.92	0.47	0.45	1.04
150	2.5	0.7	600	108.05	38.24	0.35	0.34	1.03
150	2.5	0.8	600	108.05	27.29	0.25	0.24	1.07
200	1	0.6	300	25.55	10.92	0.43	0.45	0.95
200	1	0.7	300	25.55	8.21	0.32	0.34	0.94
200	1	0.8	300	25.55	5.27	0.21	0.24	0.88
200	2	0.6	300	57.29	24.96	0.44	0.45	0.96
200	2	0.7	300	57.29	19.57	0.34	0.34	0.99
200	2	0.8	300	57.29	12.98	0.23	0.24	0.96
200	2.5	0.6	300	72.77	32.96	0.45	0.45	1.00
200	2.5	0.7	300	72.77	26.42	0.36	0.34	1.06
200	2.5	0.8	300	72.77	18.05	0.25	0.24	1.06
200	1	0.6	450	31.46	14.81	0.47	0.45	1.04
200	1	0.7	450	31.46	11.43	0.36	0.34	1.06
200	1	0.8	450	31.46	7.40	0.24	0.24	1.00

200	2	0.6	450	83.05	35.05	0.42	0.45	0.93
200	2	0.7	450	83.05	27.71	0.33	0.34	0.97
200	2	0.8	450	83.05	18.59	0.22	0.24	0.95
200	2.5	0.6	450	106.97	46.72	0.44	0.45	0.97
200	2.5	0.7	450	106.97	37.39	0.35	0.34	1.02
200	2.5	0.8	450	106.97	25.58	0.24	0.24	1.02
200	1	0.6	600	37.31	18.03	0.48	0.45	1.07
200	1	0.7	600	37.31	14.34	0.38	0.34	1.12
200	1	0.8	600	37.31	9.36	0.25	0.24	1.07
200	2	0.6	600	102.25	43.80	0.43	0.45	0.95
200	2	0.7	600	102.25	34.72	0.34	0.34	0.99
200	2	0.8	600	102.25	23.78	0.23	0.24	0.99
200	2.5	0.6	600	139.48	58.80	0.42	0.45	0.93
200	2.5	0.7	600	139.48	47.03	0.34	0.34	0.98
200	2.5	0.8	600	139.48	32.90	0.24	0.24	1.00
250	1	0.6	300	27.19	11.50	0.42	0.45	0.94
250	1	0.7	300	27.19	8.89	0.33	0.34	0.95
250	1	0.8	300	27.19	5.94	0.22	0.24	0.93
250	2	0.6	300	67.29	28.89	0.43	0.45	0.95
250	2	0.7	300	67.29	21.97	0.33	0.34	0.95
250	2	0.8	300	67.29	15.49	0.23	0.24	0.98
250	2.5	0.6	300	87.52	39.41	0.45	0.45	1.00
250	2.5	0.7	300	87.52	29.44	0.34	0.34	0.98
250	2.5	0.8	300	87.52	20.46	0.23	0.24	0.99
250	1	0.6	450	32.82	15.29	0.47	0.45	1.03
250	1	0.7	450	32.82	11.67	0.36	0.34	1.04
250	1	0.8	450	32.82	7.93	0.24	0.24	1.03
250	2	0.6	450	90.91	39.42	0.43	0.45	0.96
250	2	0.7	450	90.91	29.39	0.32	0.34	0.94
250	2	0.8	450	90.91	21.90	0.24	0.24	1.02
250	2.5	0.6	450	124.97	55.37	0.44	0.45	0.98
250	2.5	0.7	450	124.97	40.27	0.32	0.34	0.94
250	2.5	0.8	450	124.97	28.73	0.23	0.24	0.98
250	1	0.6	600	38.88	18.64	0.48	0.45	1.06
250	1	0.7	600	38.88	14.54	0.37	0.34	1.09
250	1	0.8	600	38.88	9.76	0.25	0.24	1.07
250	2	0.6	600	112.34	49.87	0.44	0.45	0.98
250	2	0.7	600	112.34	35.84	0.32	0.34	0.93
250	2	0.8	600	112.34	26.62	0.24	0.24	1.01
250	2.5	0.6	600	153.72	69.43	0.45	0.45	1.00
250	2.5	0.7	600	153.72	49.03	0.32	0.34	0.93
250	2.5	0.8	600	153.72	35.65	0.23	0.24	0.99

Mean	1.00
COV	0.06

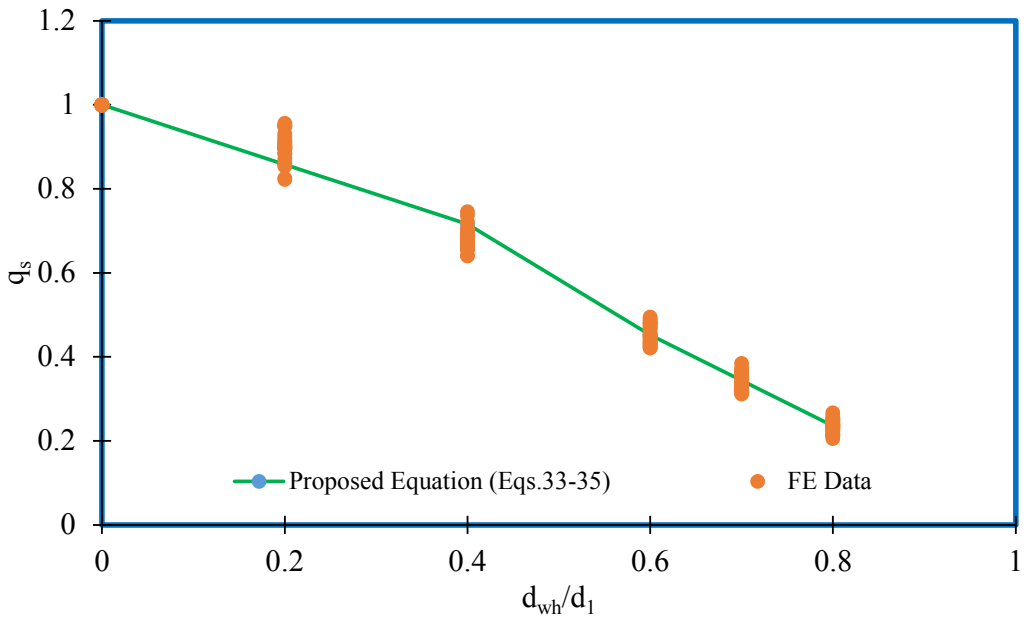

Fig. 18: Comparison of proposed equation with numerical results

6 Comparison of FE results with LCB sections

SupaCee sections are much related to LCB sections considering section profiles and lip arrangements. However, ribbed webs in SupaCee sections ensure better structural performance. This section compares similar sections of SupaCee sections and LCB sections in terms of shear behaviour. LCB sections were modelled with similar dimensions of SupaCee sections and ultimate shear capacities of LCB sections were obtained. Fig. 19 indicates the selection of LCB sections for the comparison purpose.

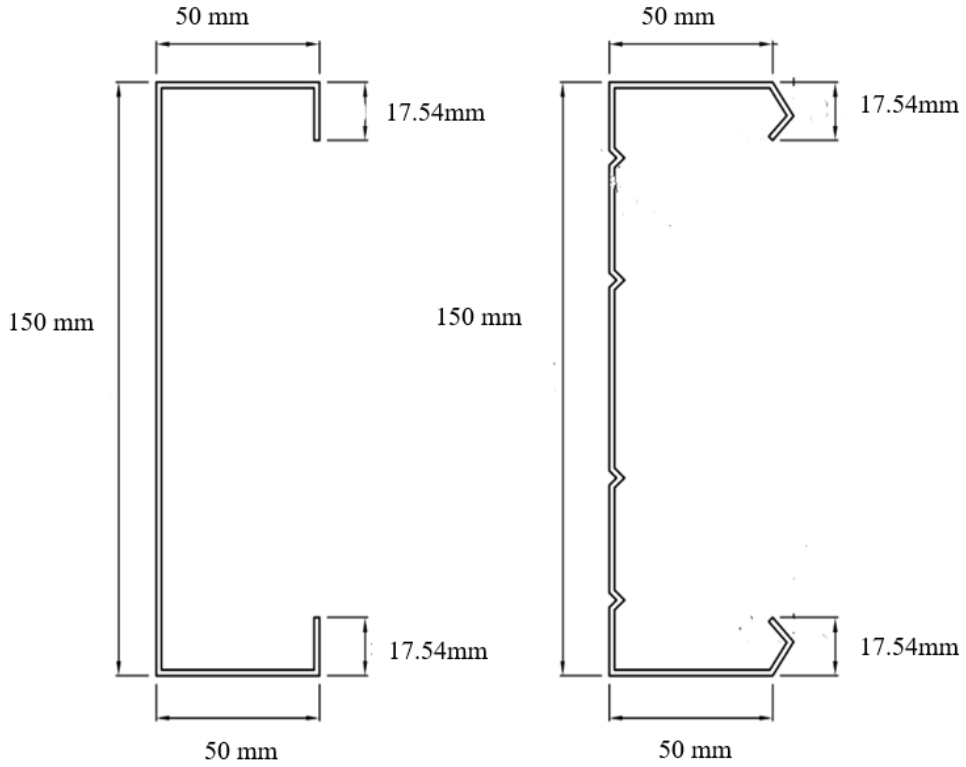

Fig.19: Dimension of LCB section for the Comparison purpose with SupaCee section

Consequently, 27 numerical models incorporating three different section depths (150 mm, 200 mm and 250 mm), three differing thicknesses (1 mm, 2 mm and 2.5 mm) and three various yield strengths (300 MPa, 450 MPa and 600 MPa) were created to replicate the same characteristics of SupaCee sections in this study. Numerical results comparison with LCB sections is stated in Table 11. The comparison revealed that shear capacity of SupaCee section is higher than LCB. Moreover, the increment percentage is decreasing when thickness increases. In this study, the increment could be observed between 3% to 30 % for considered parametric study.

Table 11. Shear capacity comparison (LCB vs SupaCee)

H (mm)	B (mm)	t (mm)	strength (MPa)	Shear capacity (kN)		Increment of SupaCee (%)
				LCB	SupaCee section	
150	50	1	300	17.09	20.38	19.25
150	50	2	300	42.09	44.27	5.18
150	50	2.5	300	53.88	56.31	4.51
150	50	1	450	23.36	29.42	25.94

150	50	2	450	61.44	64.84	5.53
150	50	2.5	450	79.27	82.38	3.92
150	50	1	600	28.22	36.84	30.55
150	50	2	600	79.45	84.81	6.75
150	50	2.5	600	103.83	108.05	4.06
200	65	1	300	19.76	25.55	29.30
200	65	2	300	54.8	57.29	4.54
200	65	2.5	300	70.05	72.77	3.88
200	65	1	450	25.48	31.46	23.47
200	65	2	450	78.94	83.05	5.20
200	65	2.5	450	102.15	106.97	4.72
200	65	1	600	30.17	37.31	23.67
200	65	2	600	95.38	102.25	7.20
200	65	2.5	600	130.69	139.48	6.73
250	75	1	300	21.36	27.19	27.29
250	75	2	300	61.74	67.29	8.99
250	75	2.5	300	82.6	87.52	5.96
250	75	1	450	26.8	32.82	22.46
250	75	2	450	84.65	90.91	7.40
250	75	2.5	450	117.28	124.97	6.56
250	75	1	600	31.43	38.88	23.70
250	75	2	600	106.62	112.34	5.36
250	75	2.5	600	148.44	153.72	3.56

Shear capacity of SupaCee section reduces with introduction of web opening and it continuously decreasing with increasing web opening size. Therefore, the shear capacity of plain LCB section was compared to the SupaCee sections with web openings (Fig. 20 to Fig. 22). Based on the comparisons, it was observed that the shear capacity of Supacee sections with web opening ratio of 0.2 ($d_{wh}/d_1 = 0.2$) is greater than the shear capacity of LCB when thickness is equal to 1 mm. For section 150x50x1 (300 MPa yield strength), Shear capacity of LCB section is 17.09 kN, whereas shear capacity of SupaCee section with web opening ratio of 0.2 is 17.4 kN. Similarly, shear capacity of SupaCee sections with web opening ratio of 0.2 is greater than the shear capacity of LCB sections for all selected same sections with 1mm thickness. However, for thicknesses of 2 mm and 2.5 mm shear capacity of LCB is slightly higher than the shear capacity of SupaCee with web opening ratio of 0.2 ($d_{wh}/d_1 = 0.2$). For sections 150x50x2 and 150x50x2.5 (300 MPa yield strength), shear capacities of LCB are 42.09 kN and 53.88 kN, whereas shear capacities of SupaCee with web opening ratio of 0.2 are 40.57 kN and 50.88 kN, respectively. Similar pattern was observed for all yield strengths and

aforementioned comparison indicates that, the increment in thickness improves the shear capacity of both LCB section and SupaCee section. However, SupaCee section has the better shear performance and the introduction of web opening affects the shear capacity when comparing to plain LCB section while increasing the thickness from 1 mm to 2.5 mm. Therefore, it can be concluded that shear capacity of CFS sections highly depends on the thickness of the web. Similar conclusions were made by Tsavdaridis and D'Mello [51-52] for steel cellular beams where the thicknesses are smaller than 7mm as the shear capacity highly depends on web thickness. Table 12 summarises the shear capacity of SupaCee section with opening size of 0.2 ($d_{wh}/d_1 = 0.2$) and shear capacity of LCB without web openings.

Based on the current study, SupaCee section with web opening ratio of 0.2 can be the replacement for plain LCB sections as the replacement will lead to regain the shear performance of LCB sections as well as the availability of web openings in order to accommodate the services. Further investigations can be conducted by changing the locations of ribs at web of SupaCee sections with openings to find out a better replacement for LCB.

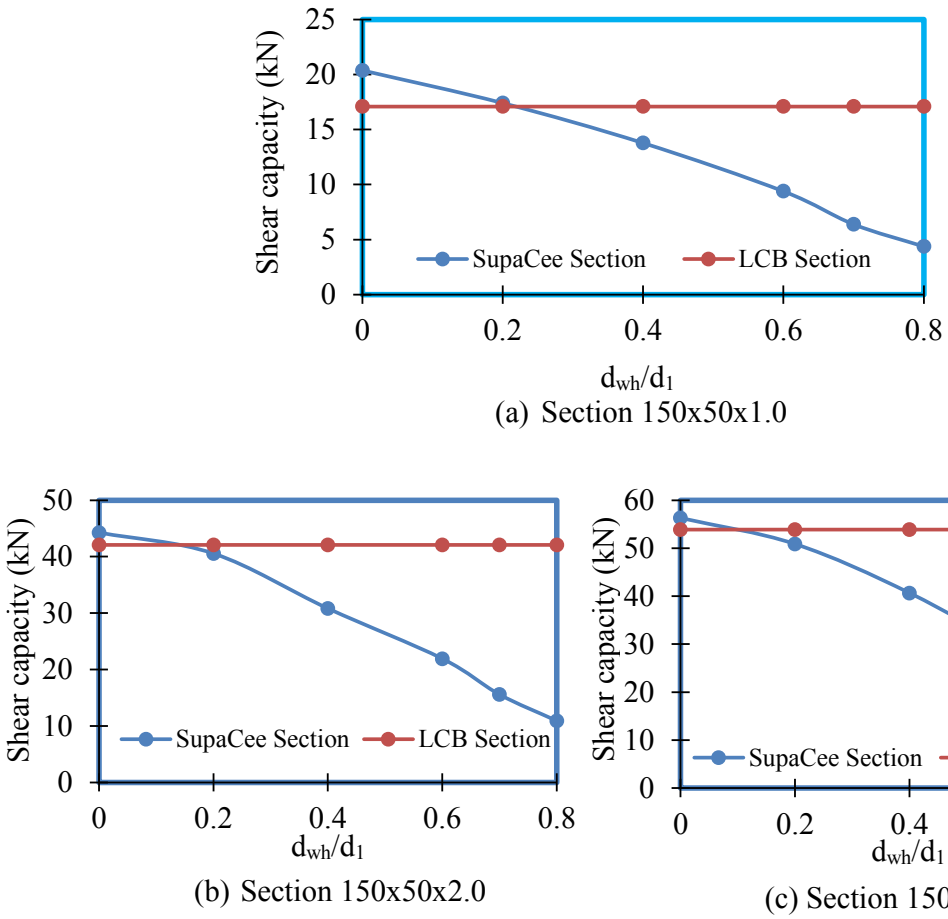

Fig. 20: Shear capacity comparison of LCB and SupaCee with web opening for section 150 section with f_y = 300 MPa

424

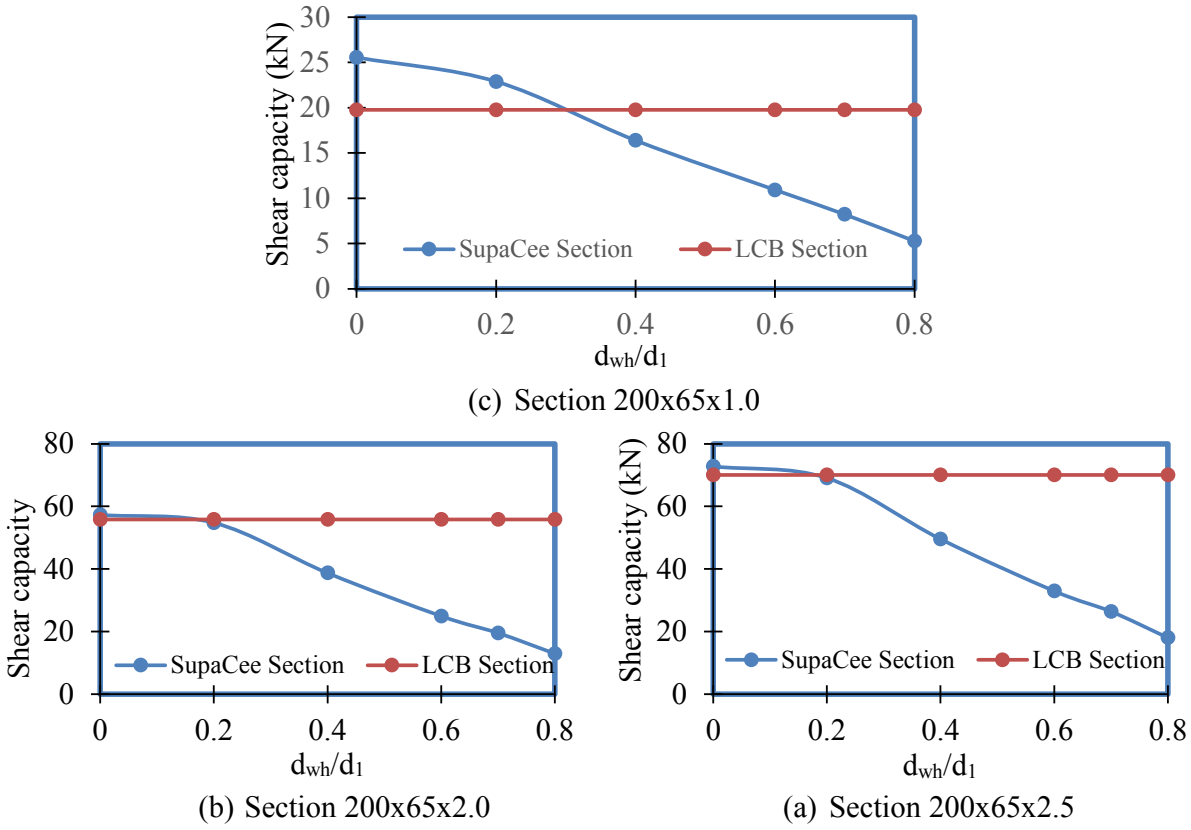

Fig. 21: Shear capacity comparison of LCB and SupaCee with web opening for section 200 section with f_y = 300 MPa

425

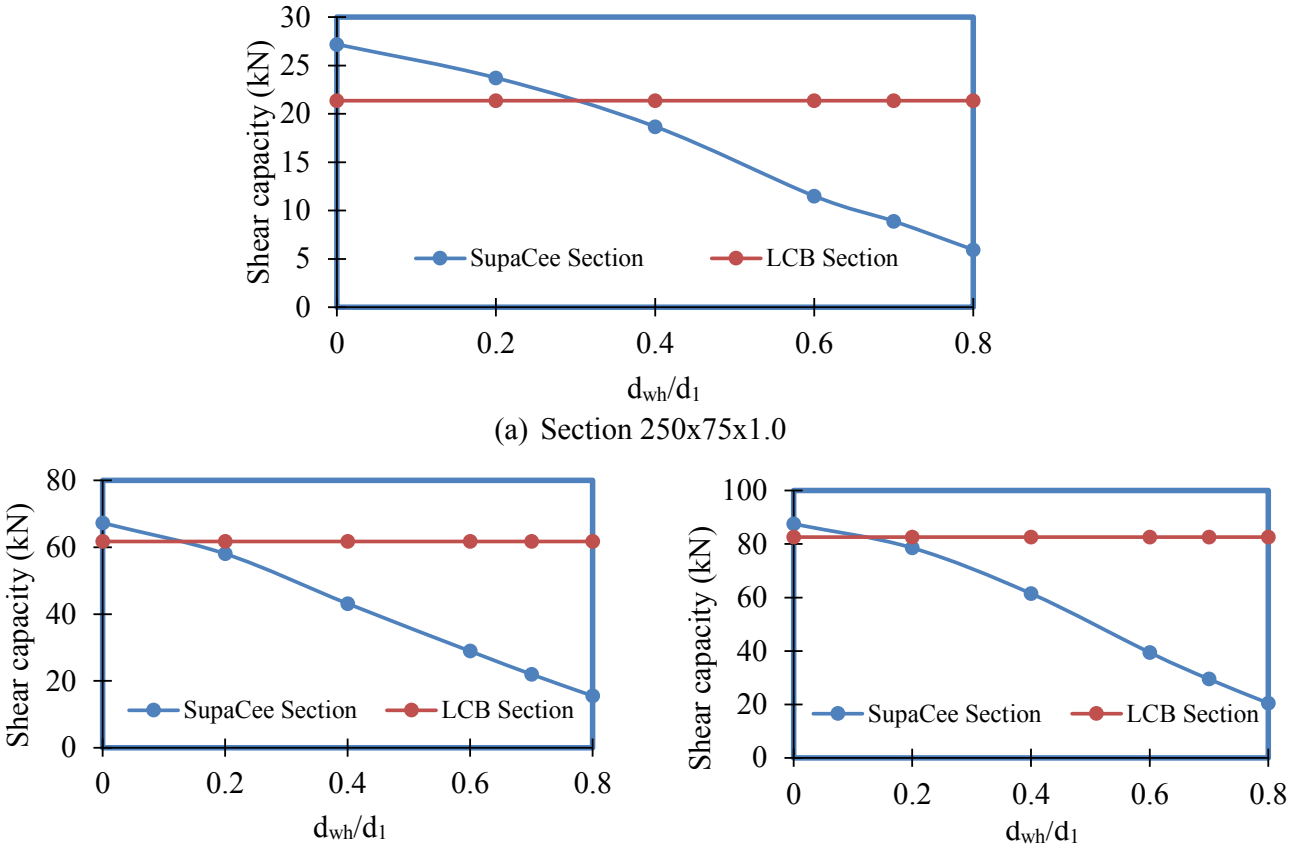

Fig. 22: Shear capacity comparison of LCB and SupaCee with web opening for section 250 section with f_y = 300 MPa

426

427 Table 12. Shear capacity comparison of LCB section with SupaCee section with openings
428 (d_{wh}/d_1 = 0.2)

Depth H (mm)	Width B (mm)	Thickness t (mm)	Yield Strength f_y (MPa)	Shear capacity (kN)		($V_{SupaCee\ with\ web\ opening\ (dwh/d1=0.2)}$ -V_{LCB})/V_{LCB} %
				LCB	SupaCee section with web opening (d_{wh}/d_1 = 0.2)	
150	50	1	300	17.09	17.40	1.81
150	50	2	300	42.09	40.57	-3.61
150	50	2.5	300	53.88	50.88	-5.57
150	50	1	450	23.36	24.29	3.98
150	50	2	450	61.44	59.11	-3.79
150	50	2.5	450	79.27	74.47	-6.06
150	50	1	600	28.22	30.32	7.44
150	50	2	600	79.45	76.23	-4.05
150	50	2.5	600	103.83	96.90	-6.67
200	65	1	300	19.76	22.88	15.79

200	65	2	300	54.82	54.77	-0.09
200	65	2.5	300	70.05	69.07	-1.40
200	65	1	450	25.48	29.90	17.35
200	65	2	450	78.94	75.72	-4.08
200	65	2.5	450	102.15	99.07	-3.02
200	65	1	600	30.17	35.53	17.77
200	65	2	600	95.38	92.80	-2.71
200	65	2.5	600	130.69	128.48	-1.69
250	75	1	300	21.36	23.72	11.05
250	75	2	300	61.74	58.05	-5.98
250	75	2.5	300	82.60	78.56	-4.89
250	75	1	450	26.80	30.57	14.07
250	75	2	450	84.65	80.40	-5.02
250	75	2.5	450	117.28	110.57	-5.72
250	75	1	600	31.43	36.88	17.34
250	75	2	600	106.62	100.61	-5.64
250	75	2.5	600	148.44	138.59	-6.64

7 Design Example

A design example is illustrated here to provide a guiding suggestion for practical engineering problems. The design example demonstrates calculation procedure based on the proposed equation in this paper, to determine the shear strength of Supacee section with openings in the web area. The openings in the web area is punched for service purposes.

(a) Given: A SupaCee section with web height (H = 150 mm), flange width (B = 50mm), thickness (t = 2.5 mm) and a circular opening with diameter of 80 mm (dwh = 80 mm) is chosen for an engineering application purposes. Moreover, the material properties are listed below.

Young's modulus = 200,000 MPa and Poisson's ratio = 0.30.

(b) Problem: Shear strength of above described SupaCee section need to be calculated.

(c) Solution: $V_{nl} = q_s V_v$

Where, V_v= nominal shear capacity, V_{nl}= shear capacity with openings, q_s= shear reduction factor

At the first step of this calculation, shear reduction factor due to the openings (qs) was calculated using proposed equation (Eqs. 33-35) and then nominal shear capacity (V_v) was calculated according to Pham and Hancock [49] study to determine the shear capacity with openings (V_{nl}). .

Step 1: This paper proposed the equation for shear strength reduction factor when openings are accommodated in the SupaCee section. Therefore, strength reduction factor was calculated first for the given problem.

As Equations are proposed in this paper (Eqs. 33-35), diameter to effective depth ratio will play a major role in predicting the shear capacity of SupaCee section with web openings and diameter to effective depth ratio was calculated.

$$0.4 < \frac{d_{wh}}{d_1} = \frac{84.6}{141} = 0.6 \leq 0.8$$

Hence, according to the proposed Equation (Eq. 35)

$$q_s = 1.10 - 1.08\left[\frac{d_{wh}}{d_1}\right] \qquad for\ 0.4 < \frac{d_{wh}}{d_1} \leq 0.8$$

$$q_s = 1.10 - (1.08 * 0.6) = 0.452$$

Step 2: Nominal shear capacity (V_v) of the SupaCee section is calculated in this step according to Pham and Hancock [49] proposed equations.

$$\lambda_v = \sqrt{V_y/V_{cr}},\ V_y = 0.6\, f_y d_1 t_w,\ V_{cr} = \frac{k_v \pi^2 E {t_w}^3}{12(1-v^2)d_1}$$

$$V_y = 0.6\, f_y d_1 t_w = 0.6 * 300 * 141 * 2.5 = 63.45 \text{ kN}$$

$$V_{cr} = \frac{k_v \pi^2 E {t_w}^3}{12(1-v^2)d_1} = \frac{12.204 * \pi^2 * 200000 * 2.5^3}{12*(1-0.3^2)* 141} = 244.461 \text{ kN}$$

$$\lambda_v = \sqrt{\frac{V_y}{V_{cr}}} = \sqrt{{63.45}/{244.461}} = 0.26 \leq 0.815$$

Since $\lambda_v = 0.26 \leq 0.815$,

$$V_v = V_y = 63.45\ kN$$

Finally, Shear capacity with openings can be calculated

$$V_{nl} = q_s V_v = 0.452 * 63.45kN = 28.68 \text{ kN}$$

From Table 5, obtained shear capacity for the section = 27.59 kN

8 Concluding Remarks

The paper has discussed the shear behaviour of SupaCee sections with web openings carrying out detailed numerical studies. Initially, numerical models were developed for the validation of experimental study. Consecutively, comprehensive parametric studies were conducted including various parameters such as thicknesses, yield strengths, section depths and web opening ratios. Overall, 162 numerical models were developed and the results were noted to

476 analyse the shear behaviour of SupaCee section with respect to aforementioned parameters.
477 The results were compared with available shear design equations for LCB sections as there are
478 no experiments on SupaCee sections with web openings. Since the comparison indicated that,
479 the available equations are inappropriate to predict the shear capacity of SupaCee sections with
480 web openings, new shear reduction factor equations were proposed based on opening depth
481 ratio factor. In addition, similar plain LCB sections were modelled to compare the results of
482 SupaCee sections with and without web openings. Comparisons indicated 3% - 30 % shear
483 capacity increment in SupaCee section. Moreover, detailed analysis was carried out to check
484 the possibilities of replacing plain LCB sections by SupaCee sections with web openings and
485 the recommendation from the analysis was stated. Therefore, this study concludes that proposed
486 equations are accurately predicting the shear capacity of SupaCee sections with web openings
487 and recommends the replacement of LCB sections by SupaCee sections with web openings
488 based on better or similar shear performance with the accommodation of service integration.

489 **Acknowledgements**

490 The authors would like to acknowledge the supports provided by the Northumbria University,
491 European research council and The Home Engineers.

492 **References**

493 [1] C.H. Pham, G.J. Hancock, Experimental Investigation and Direct Strength Design of
494 High-Strength, Complex C-Sections in Pure Bending, Journal of Structural
495 Engineering. 139 (2013) 1842–1852. https://doi.org/10.1061/(ASCE)ST.1943-
496 541X.0000736.

497 [2] L. Sundararajah, M. Mahendran, P. Keerthan, Web crippling studies of SupaCee
498 sections under two flange load cases, Engineering Structures. 153 (2017) 582–597.
499 https://doi.org/10.1016/J.ENGSTRUCT.2017.09.058.

500 [3] Pham, C. H., and Hancock, G. J. (2009). Shear Buckling of Thin-Walled Channel
501 Sections with Intermediate Web Stiffener, Proceedings, The 6th International
502 Conference on Advances in Steel Structures (ICASS2009), Hong Kong, Volume 1, pp
503 417-424.

504 [4] Pham, S. H., Pham, C. H., and Hancock, G. J. (2012). Shear Buckling of Thin-Walled
505 Channel Sections with Complex Stiffened Webs, Proceedings, the 21st International

Specialty Conference on Cold-Formed Steel Structures, Missouri University of Science & Technology, St Louis, Missouri, pp 281-262.

[5] S. Hong Pham, C.H. Pham, G.J. Hancock, Direct strength method of design for shear including sections with longitudinal web stiffeners, Thin-Walled Structures. 81 (2014) 19–28. https://doi.org/10.1016/J.TWS.2013.09.002.

[6] C. Pham, L. Bruneau, and G. Hancock, "Experimental Study of Longitudinally Stiffened Web Channels Subjected to Combined Bending and Shear," *J. Struct. Eng.*, vol. 141, p. 4015018, Feb. 2015.

[7] C. Pham and G. Hancock, "Numerical investigation of longitudinally stiffened web channels predominantly in shear," *Thin-Walled Struct.*, vol. 86, Oct. 2014.

[8] Rockey, K. C., Anderson, R. G., and Cheung, Y. K. (1969), "The Behavior of Square Shear Webs Having a Circular Hole," in Thin-Walled Steel Structures (ed. K. C. Rockey and H. V. Hill), Crosby Lockwood, London.

[9] C. H. Pham, "Shear buckling of plates and thin-walled channel sections with holes," *J. Constr. Steel Res.*, vol. 128, pp. 800–811, 2017.

[10] C. H. Pham, S. H. Pham, C. Rogers, and G. Hancock, "Shear Strength Experiments and Design of Cold-Formed Steel Channels with Web Holes," *J. Struct. Eng.*, vol. 146, p. 4019173, Jan. 2020.

[11] T. Anapayan and M. Mahendran, "Flexural behavior and design of hollow flange steel beams," Queensl. Univ. Technol., no. March, p. 435, 2010.

[12] C.H. Pham, G.J. Hancock, Numerical Simulation of High Strength Cold-Formed Supacee Sections in Combined Bending and Shear (No. R913), (2010). https://hdl.handle.net/2123/24041.

[13] C.H. Pham, G.J. Hancock, Experimental Investigation of High Strength Cold-Formed SupaCee Sections in Combined Bending and Shear (No. R907), (2009). https://hdl.handle.net/2123/24036.

[14] C. Pham, G. Hancock, Direct Strength Design of Cold-formed C-sections for Shear, in: CCFSS Proceedings of International Specialty Conference on Cold-Formed Steel Structures (1971 - 2018), 2010. https://scholarsmine.mst.edu/isccss/20iccfss/20iccfss-session5/1 (accessed July 14, 2021).

[15] C.H. Pham, G.J. Hancock, Finite Element Analyses of High Strength Cold-Formed SupaCee ® Sections in Shear, in: Proceedings of International Colloquium on Stability and Ductility of Steel Structures, Rio de Janeiro, Brazil, 2010:Volume 2, pp. 1025–1032.

[16] Australia/New Zealand Standard AS/NZS 4600 Cold-Formed Steel Structures, Standards Australia/Standards New Zealand (SA), Sydney, Australia, 2018.

[17] American Iron and Steel Institute (AISI), Specifications for the cold-formed steel structural members, cold-formed steel design manual, AISI S100, Washington DC, USA; 2016.

[18] L. Sundararajah, M. Mahendran, P. Keerthan, Design of SupaCee Sections Subject to Web Crippling under One-Flange Load Cases, Journal of Structural Engineering. 144 (2018) 04018222. https://doi.org/10.1061/(ASCE)ST.1943-541X.0002206.

[19] Dassault Systems Simulia Corp, "Abaqus/CAE 2017 User's Guide," Abaqus/CAE 520 Standard 2017. 2017.

[20] I. Fareed, W. Somadasa, K. Poologanathan, S. Gunalan, M. Corradi, and S. Sivapalan, "Finite Element Analyses of Cold-formed Stainless Steel Beam with Web Openings in Shear," ce/papers, vol. 3, no. 3–4, pp. 907–912, 2019.

[21] M.R. Haidarali, D.A. Nethercot, Finite element modelling of cold-formed steel beams under local buckling or combined local/distortional buckling, Thin-Walled Structures 49(12)(2011) 1554-1562.

[22] K. Elilarasi and B. Janarthanan, "Effect of web holes on the web crippling capacity of cold-formed LiteSteel beams under End-Two-Flange load case," Structures, vol. 25, no. September 2019, pp. 411–425, 2020.

[23] S. Hareindirasarma, K. Elilarasi, and B. Janarthanan, "Effect of circular holes on the web crippling capacity of cold-formed LiteSteel beams under Interior-Two-Flange load case," Thin-Walled Struct., vol. 166, p. 108135, 2021.

[24] D. L. Chandramohan, E. Kanthasamy, P. Gatheeshgar, K. Poologanathan, M. F. M. Ishqy, T. Suntharalingam, and T. Kajaharan, "Shear behaviour and design of doubly symmetric hollow flange beam with web openings," J. Constr. Steel Res., vol. 185, p. 106836, 2021.

[25] L. Wang, B. Young, Design of cold-formed steel channels with stiffened webs subjected to bending, Thin-Walled Structures 85 (2014) 81-92.

[26] B. W. Schafer, Z. Li, and C. D. Moen, “Computational modeling of cold-formed steel,” Thin-Walled Struct., vol. 48, no. 10–11, pp. 752–762, 2010.

[27] P. Keerthan and M. Mahendran, “Improved shear design rules for lipped channel beams with web openings,” J. Constr. Steel Res., vol. 97, pp. 127–142, 2014.

[28] M. Dissanayake, K. Poologanathan, S. Gunalan, K. D. Tsavdaridis, and B. Nagaratnam, “Finite Element Analyses of Cold-formed Stainless Steel Beams Subject to Shear,” ce/papers, vol. 3, no. 3–4, pp. 931–936, Sep. 2019.

[29] D. K. Pham, C. H. Pham, and G. J. Hancock, “Parametric study for shear design of cold-formed channels with elongated web openings,” J. Constr. Steel Res., vol. 172, p. 106222, Sep. 2020.

[30] N. Perera, M. Mahendran, Finite element analysis and design for section moment capacities of hollow flange steel plate girders, Thin-Walled Structures 135 (2019) 356-375.

[31] P. Keerthan and M. Mahendran, “Numerical Modelling of LiteSteel Beams Subject to Shear,” J. Struct. Eng., vol. 137, no. 12, pp. 1428–1439, Dec. 2011.

[32] P. Gatheeshgar, K. Poologanathan, S. Gunalan, B. Nagaratnam, K.D. Tsavdaridis, J. Ye, Structural behaviour of optimized cold-formed steel beams, Steel Construction (2020).

[33] R. Siahaan, P. Keerthan, M. Mahendran, Finite element modeling of rivet fastened rectangular hollow flange channel beams subject to local buckling, Engineering Structures 126 (2016) 311-327.

[34] G. Perampalam, K. Poologanathan, S. Gunalan, J. Ye, B. Nagaratnam, Optimum Design of Cold-formed Steel Beams: Particle Swarm Optimisation and Numerical Analysis, ce/papers 3(3-4) (2019) 205-210.

[35] P. Gatheeshgar, P. Keerthan, G. Shanmuganathan, T. Konstantinos Daniel, N. Brabha, I. Eleni, Optimised cold-formed steel beams in modular building applications, Journal of Building Engineering(2020).

595 [36] N. Degtyareva, P. Gatheeshgar, K. Poologanathan, S. Gunalan, M. Lawson, P. Sunday,
596 Combined bending and shear behaviour of slotted perforated steel channels: Numerical
597 studies, Journal of Constructional Steel Research 161 (2019) 369-384.

598 [37] P. Keerthan and M. Mahendran, "Experimental studies of the shear behaviour and
599 strength of lipped channel beams with web openings," Thin-Walled Struct., vol. 73, pp.
600 131–144, 2013.

601 [38] K. S. Wanniarachchi, M. Mahendran, and P. Keerthan, "Shear behaviour and design of
602 Lipped Channel Beams with non-circular web openings," Thin-Walled Struct., vol. 119,
603 no. September 2016, pp. 83–102, 2017.

604 [39] B. Janarthanan, K. Elilarasi, and K. Selvarajasarma, "Effect of circular openings on web
605 crippling of unlipped channel sections under end-two-flange load case," Adv. Steel
606 Constr., vol. 16, pp. 310–320, Dec. 2020.

607 [40] P. Keerthan and M. Mahendran, "Experimental studies on the shear behaviour and
608 strength of LiteSteel beams," Eng. Struct., vol. 32, no. 10, pp. 3235–3247, Oct. 2010.

609 [41] P. Keerthan and M. Mahendran, "New design rules for the shear strength of LiteSteel
610 beams," J. Constr. Steel Res., vol. 67, no. 6, pp. 1050–1063, Jun. 2011.

611 [42] P. Keerthan and M. Mahendran, "New Design Rules for the Shear Strength of LiteSteel
612 Beams with Web Openings," J. Struct. Eng., vol. 139, no. 5, pp. 640–656, May 2013.

613 [43] P. Keerthan and M. Mahendran, "Shear behaviour and strength of litesteel beams with
614 web openings," Adv. Struct. Eng., vol. 15, no. 2, pp. 171–184, 2012.

615 [44] Pham CH, Hancock GJ. Experimental investigation of high strength C-sections in
616 combined bending and shear. Journal of Structural Engineering, American Society of
617 Civil Engineers 2010; 136:866–78.

618 [45] Pham CH, Hancock GJ. Numerical simulation of high strength cold-formed purlins in
619 combined bending and shear. Journal of Constructional Steel Research2010; 66:1205–
620 17

621 [46] P. Keerthan and M. Mahendran, "Shear buckling characteristics of cold-formed steel
622 channel beams," Int. J. Steel Struct., vol. 13, no. 3, pp. 385–399, 2013.

623 [47] R. A. LaBoube, W. W. Yu, J. E. Langan, and M. Y. Shan, “Cold-formed steel webs
624 with openings: Summary report,” Thin-Walled Struct., vol. 27, no. 1, pp. 79–84, 1997.

625 [48] M. Eiler, R. LaBoube, and W. Yu, “Behavior of web elements with openings subjected
626 to linearly varying shear,” Cent. Cold-Formed Steel Struct. Libr., Jun. 1997.

627 [49] Pham CH, Hancock GJ, “School of Civil Engineering Sydney NSW 2006 Centre for
628 Advanced Structural Engineering Experimental Investigation of High Strength Cold-
629 Formed SupaCee ® Sections in Combined Bending and Shear,” no. December, 2009.

630 [50] Standards Australia. (1998). “Steel Structures.” AS/NZS 4100:1998, Standards
631 Australia/ standards New Zealand.

632 [51] Tsavdaridis, K.D. and D’Mello, C. (2011) Web Buckling Study of the Behaviour and
633 Strength of Perforated Steel Beams with Different Novel Web Opening Shapes. Journal
634 of Constructional Steel Research. 67(10), pp. 1605-1620

635 [52] Tsavdaridis, K.D. and D’Mello, C. (2012) Vierendeel Bending Study of Perforated
636 Steel Beams with Various Novel Shapes of Web Openings, through Non-Linear Finite
637 Element Analyses. Journal of Structural Engineering, ASCE. 138(10), pp. 1214-1230